CR 137963
NAS2-7613

ROTOR DYNAMIC STATE AND PARAMETER

IDENTIFICATION FROM SIMULATED

FORWARD FLIGHT TRANSIENTS

Part I of Third Yearly Report under Contract NAS2-7613

Prepared for the Ames Directorate, USAAMRDL
at Ames Research Center, Moffett Field, California

by

K. H. Hohenemser

D. Banerjee

S. K. Yin

Department of Mechanical Engineering

Washington University

School of Engineering and Applied Science

St. Louis, Missouri 63130

June 1976

ROTOR DYNAMIC STATE AND PARAMETER

IDENTIFICATION FROM SIMULATED

FORWARD FLIGHT TRANSIENTS

Part I of Third Yearly Report under Contract NAS2-7613
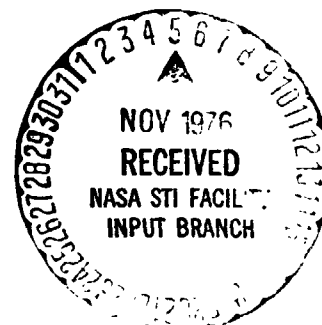
by

K. H. Hohenemser

D. Banerjee

S. K. Yin

Department of Mechanical Engineering

Washington University

School of Engineering and Applied Science

St. Louis, Missouri 63130

June 1976

Preface to Third Yearly Report under Contract NAS2-7613

Work under Contract NAS2-7613 started on July 1, 1973. The research goals for a 3 year period stated in this contract are:

(a) Assess analytically the effects of fuselage motions on stability and random response. The problem is to develop an adequate but not overly complex flight dynamics analytical model and to study the effects of structural and electronic feedback, particularly for hingeless rotors.

(b) Study by computer and hardware experiments the feasibility of adequate perturbation models from non-linear trim conditions. The problem is to extract an adequate linear perturbation model for the purpose of stability and random motion studies. The extraction is to be performed on the basis of transient responses obtained either by computed time histories or by model tests.

(c) Extend the experimental methods to assess rotor wake-blade interactions by using a 4-bladed rotor model with the capability of progressing and regressing blade pitch excitation (cyclic pitch stirring), by using a 4-bladed rotor model with hub tilt stirring, and by testing rotor models in sinusoidal up or side flow.

Seven reports on the work under Contract NAS2-7613 have been submitted, references 1 to 7. Reference 1 completes research goal (a). References 2, 4, 6, 7 pertain to research goal (b). It is incomplete to date. References 3 and 5 pertain to research goal (c). It also is incomplete to date. Reference 3 presents the results of extensive frequency response tests. Reference 5 presents dynamic downwash

measurements in hovering during harmonic rotor excitation. Three
manuscripts for publication have been prepared. The first has been
published as reference 8. Two further manuscripts covering part of
the material in references 3 and 7 have been submitted to journals.

The extensive rotor state and parameter identification work with
computer simulated transients was found to be very useful for the
subsequent data processing of the measured transients. It allowed to
sort out possible inadequacies of the applied identification algorithm
and of the inputs from possible inadequacies of the measurements and
of the applied mathematical rotor model. Rotor state and parameter
identifications from measured transients are presently complete for
hovering conditions using cyclic pitch stirring transients. They are
presented in reference 7. The corresponding work for forward flight
conditions and for hub tilt stirring is planned to be completed in
FY 1977 during an authorized extension of the research contract. It
is also planned to refine the analytical rotor model used for the
state and parameter identifications to include blade flexibility.

Rotor state and parameter identification from transients is still
a field where little experience is available. As elaborated in
Chapter ⊥ of reference 4 it takes four important ingredients to perform
a successful state and parameter identification from transients; a
suitable input, a suitable instrumentation for measuring key state
variables, an adequate mathematical model of the system, and an
efficient criterion function for the estimation algorithm. In all
four respects considerable work had to be done in order to finally
establish a combination of these four ingredients that led to success.

The lessons learned in this effort are hoped to pave the way for a wider application of rotor dynamic perturbation state and parameter identifications from transients about non-linear trim conditions, both in rotor wind tunnel testing and in rotor flight testing.

Rotor Dynamic State and Parameter Identification From

Simulated Forward Flight Transients

K. H. Hohenemser, D. Banerjee, and S. K. Yin

Abstract

State and parameter identifications from simulated forward flight
blade flapping measurements are presented. The transients are
excited by progressing cyclic pitch stirring or by hub stirring with
constant stirring acceleration. Rotor dynamic inflow models of
varying degree of sophistication are used from a one parameter inflow
model (equivalent Lock number) to an eight parameter inflow model.
The maximum likelihood method with assumed fixed measurement error
covariance matrix is applied. The rotor system equations for both
fixed hub and tilting hub are given. The identified models are
verified by comparing true responses with predicted responses. An
optimum utilization of the simulated measurement data can be defined.
From the numerical results it can be anticipated that brief periods of
either accelerated cyclic pitch stirring or of hub stirring are
sufficient to extract with adequate accuracy up to 8 rotor dynamic
inflow parameters plus the blade Lock number from the transients.

v

Table of Contents

1

Notation

B	blade tip loss factor
F, F'	rotor state matrices of size 8 x 8 and 11 x 11 respectively
G_v, G_u	matrices relating induced flow and control variables respectively to the rates of states
J	criterion function
L	rotor induced flow gain matrix
M, N_v, N_u	matrices relating the state, induced flow and control variables respectively to the rotor thrust and moment coefficients
M	information matrix
P_1, ... P_5	rotor induced flow parameters
P	blade natural flapping frequency
R	measurement error covariance matrix
a	blade section lift slope
C_T	rotor thrust coefficient, positive up
C_M	rotor pitching moment coefficient, positive nose-up
C_L	rotor rolling moment coefficient, positive to right
t	non-dimensional time (period of revolution 2π)
t_k	time it takes kth blade to move from rear position to present position
u	control vector
v	total mean rotor flow velocity (non-dimensional), or noise vector
x	rotor state vector
y	rotor measurement vector
α_k	hub tilting angle at kth blade, positive up

Notation (continued)

α_I	nose down hub tilting angle
α_{II}	left hub tilting angle
β_k	flapping angle of kth blade, positive up
β_I	nose down cyclic flapping angle
β_{II}	left cyclic flapping angle
β_d	blade differential coning angle
γ	blade Lock number
θ_k	pitch angle of kth blade, positive nose up
θ_I	nose down cyclic pitch angle
θ_{II}	left cyclic pitch angle
θ_o	collective pitch angle
μ	rotor advance ratio
$\overline{\lambda}$	total mean rotor inflow velocity
$\overline{\nu}$	rotor mean induced velocity
ν_o	mean perturbation induced velocity

non-dimensional positive down

ν_I	perturbation cyclic induced velocity at blade tip, down at rear
ν_I	perturbation cyclic induced velocity at blade tip, down at right
σ	rotor solidity ratio, or standard deviation

Superscripts

$\cdot$	time differentiation
$\char`\^$	estimated value
T	transposed matrix
*	equivalent

Subscripts

m	measured variable
E	empirical

Introduction

This report covers the extension of computer simulation work pre-
sented in references 2 and 4. Reference 2 refers to rotor dynamic
state and parameter identifications in forward flight (.4 advance ratio)
using the concept of an equivalent Lock number to approximate rotor
dynamic inflow effects. Two analytical models were used; a complete
single blade representation in the rotating frame of reference, and a
simplified multiblade representation omitting periodic terms and
omitting multiblade accelerations. Two parameters were identified from
the simulated noise polluted blade flapping measurements; the equivalent
Lock number, and the collective pitch angle. Two transient inputs were
studied; a rectangular normal flow pulse, and a wave shaped normal flow
pulse. The simulated measurements with computer generated noise
pollution were first preprocessed by either a digital filter that took
out the high frequency noise or by a Kalman filter that used estimates
of the unknown parameters. The parameters were identified by integrating
a set of differential equations that sequentially minimized the system
equation error. The unknown parameters could be particularly well
retrieved for the wave shaped normal flow pulse. This was true both for
the single blade model with periodic coefficients and for the approximate
multiblade model with omitted periodic terms and accelerations.

Reference 4, Chapter 2, refers to rotor state and parameter
identifications both in forward flight and in hovering using cyclic
pitch stirring transients as inputs. The forward flight model was
limited to the concept of equivalent Lock number, either in the form of

a single blade representation with periodic coefficients, or in the
form of a multiblade representation with constant coefficients. The
simulated measurements were again polluted by computer generated
noise. The method used in reference 2 was modified in two ways; first,
instead of the sequential equation error minimization, a global
equation error minimization was used that is computationally more
efficient; second, the Kalman filter to preprocess the measurements
was used in an iterative way, being updated whenever new parameter
estimates were available. The iterated equation error estimation with
updated Kalman filter was compared with a version of the so called
maximum likelihood method where system noise is not modeled. It was
found that despite somewhat more computer CPU time per iteration, the
maximum likelihood method was superior because of more rapid convergence
and because of more meaningful parameter covariances.

The maximum likelihood method was then applied to the problem of
rotor dynamic state and parameter identification from cyclic pitch
stirring transients in hovering using a time delayed rotor inflow.
Now 3 parameters were assumed to be unknown; the blade Lock number, the
inflow gain, and the inflow time constant. Two inputs were assumed.
At time zero a step input in cyclic pitch, and at time t = 70 the
beginning of cyclic pitch stirring with constant stirring acceleration.
The identification process was started at t = 70. The transient from
the step input had not completely subsided when cyclic pitch stirring
began. It was found necessary to include the initial values of the
blade flapping deflection and of the rotor inflow as unknowns in the
parameter identification scheme, leading to 7 unknown parameters.

Though this required 6.3 CPU seconds per iteration, (IBM 360/65 computer) the second iteration was found to be almost converged, so that the total computer effort was moderate. For the tests there is no step input of cyclic pitch, so that initial value identifications can be omitted.

Reference 4, Chapter 3 develops a method of estimating the optimum transient data length that proved to be later very useful in all state and parameter identifications. In the maximum likelihood method one needs the inverse of the so-called information matrix that theoretically gives lower bounds to the parameter covariances. A differential equation for the inverted information matrix was derived and it was found that its integration results in the definition of a data length beyond which no improvement to the parameter covariances can be expected. If less data are used in the identification, a rapid increase in the parameter covariances occurs. Thus a rational way was found to avoid errors from insufficient data length and to avoid unnecessary computer effort and a degradation of accuracy from meaningless additional data.

As mentioned before, the forward flight studies in references 2 and 4 were limited to the concept of equivalent Lock number. What remains is to apply the concept of a time delayed rotor inflow to forward flight conditions and to also consider rotor hub stirring transients mentioned in research goal (c). Computer simulations were performed to study the feasibility of these types of application of the maximum likelihood method. The present report describes this work.

Single Blade and Mult·blade Coordinates

As before, the numerical analysis is performed for an advance ratio of .4. Since now dynamic rotor inflow that couples the motions of the various blades is included, a multiblade representation is called for. The relations between single blade and multiblade variables are:

Blade flapping angle: $\beta_k = \beta_0 + \beta_d(-1)^{k-1} + \beta_I \cos t_k + \beta_{II} \sin t_k$

Blade pitch angle: $\theta_k = \theta_0 - \theta_I \sin t_k + \theta_{II} \cos t_k$ (1)

Induced flow: $\nu_k = \nu_0 + \nu_I(r/R)\cos t_k + \nu_{II}(r/R)\sin t_k$

The subscript I refers to forward cyclic flapping, cyclic pitch and cyclic induced flow (the inflow is down in the rear), the subscript II refers to left cyclic flapping, cyclic pitch and cyclic induced flow (the inflow is down to the right). β_d represents differential coning for the 4-bladed rotor, whereby one pair of opposing blades cones up, the other pair cones down. Though a linear distribution of the induced flow over the radius is defined in Eq. (1), this assumption is not required for the parameter identification process. Different inflow distributions merely produce different values in the identified parameters but do not change the form of the equations.

For the tests the constant collective blade pitch θ_0 is known. Also known are the cyclic blade pitch variables $\theta_I(t)$, $\theta_{II}(t)$ as function of time. The only measured state variables are the 4 blade flapping angles β_{1m}, β_{2m}, β_{3m}, β_{4m}. As can be derived from Eq. (1) the multiblade flapping variables are related to the single blade flapping variables by the transformation

$$
\begin{bmatrix} \beta_0 \\ \beta_I \\ \beta_{II} \\ \beta_d \end{bmatrix} = (1/4) \begin{bmatrix} 1 & 1 & 1 & 1 \\ 2\cos t & -2\sin t & -2\cos t & 2\sin t \\ 2\sin t & 2\cos t & -2\sin t & -2\cos t \\ 1 & -1 & 1 & -1 \end{bmatrix} \begin{bmatrix} \beta_1 \\ \beta_2 \\ \beta_3 \\ \beta_4 \end{bmatrix} \tag{2}
$$

with its inverse

$$
\begin{bmatrix} \beta_1 \\ \beta_2 \\ \beta_3 \\ \beta_4 \end{bmatrix} = \begin{bmatrix} 1 & \cos t & \sin t & 1 \\ 1 & -\sin t & \cos t & -1 \\ 1 & -\cos t & -\sin t & 1 \\ 1 & \sin t & -\cos t & -1 \end{bmatrix} \begin{bmatrix} \beta_0 \\ \beta_I \\ \beta_{II} \\ \beta_d \end{bmatrix} \tag{3}
$$

For the computer simulations it was assumed that there is additive noise in the single blade flapping measurements. Thus the measurement equations are

$$
\begin{bmatrix} \beta_{1m} \\ \beta_{2m} \\ \beta_{3m} \\ \beta_{4m} \end{bmatrix} = \begin{bmatrix} 1 & \cos t & \sin t & 1 \\ 1 & -\sin t & \cos t & -1 \\ 1 & -\cos t & -\sin t & 1 \\ 1 & \sin t & -\cos t & -1 \end{bmatrix} \begin{bmatrix} \beta_0 \\ \beta_I \\ \beta_{II} \\ \beta_d \end{bmatrix} + \begin{bmatrix} v_1 \\ v_2 \\ v_3 \\ v_4 \end{bmatrix} \tag{4}
$$

The measurement noise covariance R was assumed to be given and not changed during the iterations. The innovation is given by (see Chapter 2 of reference 4)

$$
v = \begin{bmatrix} \beta_{1m} - \hat{\beta}_1 \\ \beta_{2m} - \hat{\beta}_2 \\ \beta_{3m} - \hat{\beta}_3 \\ \beta_{4m} - \hat{\beta}_4 \end{bmatrix} \tag{5}
$$

In order to determine the estimates $\hat{\beta}_1$, $\hat{\beta}_2$, $\hat{\beta}_3$, $\hat{\beta}_4$ from the estimates for the multiblade coordinates $\hat{\beta}_0$, $\hat{\beta}_I$, $\hat{\beta}_{II}$, $\hat{\beta}_d$ one needs Eq. (3).

For the state and parameter identifications from test data a slightly different procedure was selected, as discussed in reference 7. The measurements β_{1m}, β_{2m}, β_{3m}, β_{4m} were first transformed to multiblade coordinates by using Eq. (2). These multiblade variables β_{om}, β_{Im}, β_{IIm}, β_{dm} were then considered in the estimation algorithm as measured quantities with additive noise:

$$
\begin{bmatrix} \beta_{om} \\ \beta_{Im} \\ \beta_{IIm} \\ \beta_{dm} \end{bmatrix}
=
\begin{bmatrix} \beta_o + v_o \\ \beta_I + v_I \\ \beta_{II} + v_{II} \\ \beta_d + v_d \end{bmatrix}
\tag{6}
$$

The innovation vector is then given by

$$
v =
\begin{bmatrix} \beta_{om} - \hat{\beta}_o \\ \beta_{Im} - \hat{\beta}_I \\ \beta_{IIm} - \hat{\beta}_{II} \\ \beta_{dm} - \hat{\beta}_d \end{bmatrix}
\tag{7}
$$

The measurement error covariance was not considered given but was updated in each iteration. The procedure used for the state and parameter identifications from test data has the advantage of saving for each iteration the execution of the transformation Eq. (3). Also in this procedure suitable weights are applied to the test data in the

form of the measurement error covariance determined from the preceding iteration.

Inflow Model with One Time Constant

We adopt here the rotor inflow model of references 9 and 10. Eq. (33) of reference 10, written in our notation, reads

$$\frac{1}{\sigma a} \begin{bmatrix} k_m & 0 & 0 \\ 0 & -k_I & 0 \\ 0 & 0 & -k_I \end{bmatrix} \begin{bmatrix} \dot{v}_o \\ \dot{v}_I \\ \dot{v}_{II} \end{bmatrix} + [L_E]^{-1} \begin{bmatrix} v_o \\ v_I \\ v_{II} \end{bmatrix} = \frac{1}{\sigma a} \begin{bmatrix} C_T \\ C_M \\ C_L \end{bmatrix} \tag{8}$$

Rotor thrust and moment coefficients C_T, C_M, C_L are from aerodynamic contributions only. L_E is the empirical L-matrix defined in reference 9. The theoretical values of k_m and k_I, using potential flow around a solid disk are given in reference 10 as $k_m = .849$, $k_I = .113$. The components of the L-matrix as well as k_m and k_I will be identified from rotor transient tests. From momentum theory one obtains according to reference 10

$$[L]^{-1} = \frac{1}{\sigma a} \begin{bmatrix} 2v & 0 & 0 \\ 0 & -v/2 & 0 \\ 0 & 0 & -v/2 \end{bmatrix} \tag{9}$$

with

$$v = \frac{\mu^2 + \overline{\lambda}(\overline{\lambda} + \overline{v})}{(\mu^2 + \overline{\lambda}^2)^{1/2}} \tag{10}$$

where $\overline{\lambda}$ and $\overline{v}$ are the trim values, about which the rotor inflow perturbations v_o, v_I, v_{II} are taken. Note that an induced flow

trim value is only defined with respect to the axial induced flow. For the pitch stirring rotor model we have prior to the start of the pitch stirring transient a cyclic pitch trim condition equal to the amplitude of the cyclic pitch stirring. This amplitude is considered to be a linear perturbation variable and not part of a non-linear trim condition.

For steady conditions at advance ratio .4 one obtains from reference 9

$$
\begin{bmatrix} v_O \\ v_I \\ v_{II} \end{bmatrix} = \frac{1}{\mu} \begin{bmatrix} .5 & 0 & 0 \\ 0 & -2.0 & -1.0 \\ 0 & 1.0 & -3.0 \end{bmatrix} \begin{bmatrix} c_T \\ c_M \\ c_L \end{bmatrix} \tag{11}
$$

In reference 9 cyclic induced inflow was assumed with constant distribution over the radius. To adjust for the linear distribution assumed in reference 10 and in Eq. (1) the empirical L-matrix given in Eq. (11) is changed to

$$
L_E = \frac{1}{\mu} \begin{bmatrix} .5 & 0 & 0 \\ 0 & -2.7 & -1.3 \\ 0 & 1.3 & -4.0 \end{bmatrix} \tag{12}
$$

After inversion of this matrix, division by k_m and k_I, insertion of $\mu = .4$ and rounding off the numbers, one obtains Eq. (8) in the form

$$\begin{bmatrix} \dot{\nu}_O \\ \dot{\nu}_I \\ \dot{\nu}_{II} \end{bmatrix} + \begin{bmatrix} 1.00 & 0 & 0 \\ 0 & 1.2 & -.4 \\ 0 & .4 & .8 \end{bmatrix} \begin{bmatrix} \nu_O \\ \nu_I \\ \nu_{II} \end{bmatrix} = 1.2 \begin{bmatrix} C_T \\ -7.5\ C_M \\ -7.5\ C_L \end{bmatrix} \tag{13}$$

The rotor moment coefficients C_M and C_L are here assumed with their usual sign, positive when the moments from the flow on the rotor are nose-up and to the right respectively.

Three types of state and parameter identification from computer simulated measurements were performed. In the most general case there are 8 unknown inflow parameters in Eq. (13):

$$\begin{bmatrix} \dot{\nu}_O \\ \dot{\nu}_I \\ \dot{\nu}_{II} \end{bmatrix} + \begin{bmatrix} P_1 & 0 & 0 \\ 0 & P_2 & P_3 \\ 0 & P_4 & P_5 \end{bmatrix} \begin{bmatrix} \nu_O \\ \nu_I \\ \nu_{II} \end{bmatrix} = \begin{bmatrix} \tau_O\ C_T \\ -\tau_I\ C_M \\ -\tau_{II}\ C_L \end{bmatrix} \tag{14}$$

The 5 parameters P_1 to P_5 represent inflow gain constants, while τ_O, τ_I, τ_{II} are time constants. In this form no assumption is made about the relations between the 3 time constants.

In the second case the theoretical relations $\tau_I = \tau_{II} = 7.5\ \tau_O$ from reference 10 are used. This reduces the number of unknown inflow parameters from 8 to 6:

$$\begin{bmatrix} \dot{\nu}_O \\ \dot{\nu}_I \\ \dot{\nu}_{II} \end{bmatrix} + \begin{bmatrix} P_1 & 0 & 0 \\ 0 & P_2 & P_3 \\ 0 & P_4 & P_5 \end{bmatrix} \begin{bmatrix} \nu_O \\ \nu_I \\ \nu_{II} \end{bmatrix} = \tau \begin{bmatrix} C_T \\ -7.5\ C_M \\ -7.5\ C_L \end{bmatrix} \tag{15}$$

In the third case only diagonal terms are retained in the inflow gain matrix so that $P_4 = P_3 = 0$. This further reduces the number of unknown parameters from 6 to 4. The inflow gain parameters and the inflow time constants will depend on the trim condition and on the rotor advance ratio μ .

Rotor System Equations, Fixed Hub

The rotor system equations are written in the form

$$\dot{x} = Fx + G_\nu \, \nu + G_u \, u \tag{16}$$

with the state vector x given by

$$x^T = [\beta_o \dot{\beta}_o \beta_I \dot{\beta}_I \beta_{II} \dot{\beta}_{II} \beta_d \dot{\beta}_d] \tag{17}$$

with the induced flow vector given by $\quad \nu^T = [\nu_o \nu_I \nu_{II}] \tag{18}$

and with the control vector given by $\quad u^T = [\theta_o \theta_I \theta_{II}] \tag{19}$

Finally we have a set of equations that gives the aerodynamic thrust and moment coefficients in terms of state vector x, inflow vector ν and control vector u:

$$\begin{bmatrix} C_T/(a\sigma/2) \\ C_M/(a\sigma/2) \\ C_L/(a\sigma/2) \end{bmatrix} = Mx + N_\nu \, \nu + N_u \, u \tag{20}$$

The matrices F, G_ν, G_u, M, N_ν, N_u are respectively of size 8 x 8, 8 x 3, 8 x 3, 3 x 8, 3 x 3, 3 x 3. For moderate advance ratio neglecting reversed flow effects and assuming 4 straight constant chord blades hinged at the rotor center, these 6 matrixes are:

F-Matrix ($F_1 = B^4\gamma/8$; $F_2 = B^3\gamma\,\mu/12$, $F_3 = B^2\gamma\,\mu^2/16$)

0	1	0	0	0	0	0
$-P^2$	$-F_1$	0	0	$-F_2$	$-2F_3\sin 2t$	0
0	0	1	0	0	$-2F_2\cos 2t$	0
$-2F_2$	0	$-F_1$	$-F_1-F_3(1-\cos 4t)$	-2	$-2F_2\cos 2t$	$-2F_2\sin 2t$
0	$-2F_2$	0	$1-P^2+F_3\sin 4t$	1	$-2F_2\sin 2t$	0
0	0	2	0	$-F_1$	0	1
0	0	0	0	0	0	$-F_1$
$-2F_3\sin 2t$	0	$-F_2\sin 2t$	$-2F_2\sin 2t$	$F_2\cos 2t$	$-P^2$	$-F_1$

Additional column:

0	0
0	0
1	0
$-F_1$	$1-P^2-F_3\sin 4t$
0	$F_1-F_3(1-\cos 4t)$
2	0
0	0
$-F_2\sin 2t$	$-2F_2\cos 2t$

Gᵥ – Matrix

0	0	0
$-B^3\gamma/6$	0	$-F_2$
0	0	0
0	$-F_1$	0
$-B^2\gamma\mu/4$	0	0
0	0	$-F_1$
0	0	0
0	$-F_2\sin 2t$	$F_2\cos 2t$

G_u – Matrix for Pitch Stirring

0	0	0
F_1+2F_3	$-2F_2$	0
0	0	0
0	$F_3\sin 4t$	$F_1+F_3(1-\cos 4t)$
$4F_2$	0	0
0	$-F_1-F_3(3+\cos 4t)$	$-F_3\sin 4t$
$-2F_3\cos 2t$	0	0
	$2F_2\cos 2t$	$2F_2\sin 2t$

M – Matrix ($M_1 = B^2\mu^2/8$, $M_2 = B^3\mu/3$)

0	$-B^3/3$	0	0	$-B^2\mu/4$	$-(B\mu^2/2)\sin 2t$	0
M_2	0	$M_1 \sin 4t$	$B^4/4 + M_1(1-\cos 4t)$	0	$M_2 \cos 2t$	$M_2 \sin 2t$
0	M_2	$-B^4/4 + M_1(1-\cos 4t)$	$-M_1 \sin 4t$	$B^4/4$	$M_2 \sin 2t$	$-M_2 \cos 2t$

N_ν – Matrix

$-B^2/2$	0	$-B^2\mu/4$
0	$B^4/4$	0
$B^2\mu/2$	0	$B^4/4$

N_μ – Matrix

$(B^3/3)+B\mu/2$	$-B^2\mu/2$	0
0	$-M_1 \sin 4t$	$-B^4/4 - M_1(1-\cos 4t)$
$-2B^3\mu/3$	$B^4/4 + M_1(3+\cos 4t)$	$M_1 \sin 4t$

When inserting Eq.(8) into Eq. (20) the rotor thrust and moment κ i ficients are eliminated and one obtains a system equation of the $\llcorner$ .rm

$$\dot{x} = F' \; x + Gu \tag{21}$$

where the state vector now includes the inflow variables

$$x^T = [\beta_o \dot{\beta}_o \beta_I \dot{\beta}_I \beta_{II} \dot{\beta}_{II} \beta_d \dot{\beta}_d \nu_o \nu_I \nu_{II}] \tag{22}$$

where the state matrix F' is of size 11 x 11, and where the control matrix G is of size 11 x 3. Note that in the state and parameter identifications only 4 out of the 11 state variables are measured.

In addition to the inflow parameters the rotor system equations have as parameters the advance ratio μ that can be considered known, the Lock number γ and the tip loss factor B. In principle both γ and B could be identified from the transient test results. We usually set B = .97 and then identified γ. The system equations also contain the blade natural frequency when rotating P that could be easily identified from transient test data. In many identifications we assumed P as a known quantity. The assumptions made in deriving the system equations are less restrictive than they may appear. Only the form of the equations is used in the state and parameter identification procedure. All parameters are left open and are adapted to the test results in such a way that the quadratic differences between predicted and actual measurements are minimized.

Rotor System Equations, Tilting Hub

As defined in Research Goal (c) transient rotor testing toward establishing dynamic rotor wake-blade interactions is to be performed both with cyclic pitch stirring and with hub tilt stirring. A second

rotor model with the capability of hub tilt stirring is being built.
The rotor system equations on which the state and parameter identi-
fications will be based are described in the following.

The second of Eqs. (1) is now replaced by

$$\alpha_k = \alpha_I \cos t_k + \alpha_{II} \sin t_k \tag{23}$$

where α_I and α_{II} are the forward and left hub tilting angle
respectively. The blades are again assumed straight and elasticly
hinged at the rotor center. The blade flapping angles $\beta_1 \cdots \beta_4$ and
the associated multiblade angles β_I, β_{II} are defined <u>not</u> with respect
to the hub but rather with respect to the space fixed reference rotor
plane for zero hub tilting angle. Hub tilting α_I and α_{II} has the
same effect as cyclic pitch application θ_I and θ_{II}, except for the
elastic blade restraining moments that are opposite those from β_I
and β_{II}. Thus the control vector is now given by

$$u^T = [\theta_o \ \alpha_I \ \alpha_{II}] \tag{24}$$

instead of by Eq. (19), and elastic restraint terms must be added to
the G_u - Matrix, since the elastic pitching and rolling moments are
now proportional to $\beta_I - \alpha_I$ and $\beta_{II} - \alpha_{II}$ respectively instead of
proportional to β_I and β_{II}.

G_u - Matrix for Hub Stirring

0	0	0
$F_1 + 2 F_3$	$-2F_2$	0
0	0	0
0	$P^2 - 1 + F_3 \sin 4t$	$F_1 + F_3(1 - \cos 4t)$
0	0	0
$4F_2$	$-F_1 - F_3(3 + \cos 4t)$	$P^2 - 1 - F_3 \sin 4t$
0	0	0
$-2F_3 \cos 2t$	$2F_2 \cos 2t$	$2F_2 \sin 2t$

In all other respects Eqs. (16) to (22) including the expressions for the remaining 5 matrices remain unchanged, though the flapping angles are now defined differently as compared to the hub-fixed case.

The measurement equations (4) are now different since the blade flapping angles are measured with respect to the hub. For the computer simulations we have instead of Eq. (4) the measurement equations:

$$\begin{bmatrix} (\beta_1 - \alpha_1)_m \\ (\beta_2 - \alpha_2)_m \\ (\beta_3 - \alpha_3)_m \\ (\beta_4 - \alpha_4)_m \end{bmatrix} = \begin{bmatrix} 1 & \cos t & \sin t & 1 \\ 1 & -\sin t & \cos t & -1 \\ 1 & -\cos t & -\sin t & 1 \\ 1 & \sin t & -\cos t & -1 \end{bmatrix} \begin{bmatrix} \beta_o \\ \beta_I - \alpha_I \\ \beta_{II} - \alpha_{II} \\ \beta_d \end{bmatrix} + \begin{bmatrix} v_1 \\ v_2 \\ v_3 \\ v_4 \end{bmatrix} \qquad (25)$$

The innovation is given, instead of by Eq. (5), by

$$\nu = \begin{bmatrix} (\beta_1 - \alpha_1)_m - (\hat{\beta}_1 - \alpha_1) \\ (\beta_2 - \alpha_2)_m - (\hat{\beta}_2 - \alpha_2) \\ (\beta_3 - \alpha_3)_m - (\hat{\beta}_3 - \alpha_3) \\ (\beta_4 - \alpha_4)_m - (\hat{\beta}_4 - \alpha_4) \end{bmatrix} \qquad (26)$$

For the state and parameter identifications from test data a somewhat different procedure will be followed, whereby the single blade measurements are first transformed into multiblade measurements:

$$\begin{bmatrix} \beta_{om} \\ (\beta_I - \alpha_I)_m \\ (\beta_{II} - \alpha_{II})_m \\ \beta_{dm} \end{bmatrix} = (1/4) \begin{bmatrix} 1 & 1 & 1 & 1 \\ 2\cos t & -2\sin t & -2\cos t & 2\sin t \\ 2\sin t & 2\cos t & -2\sin t & -2\cos t \\ 1 & -1 & 1 & -1 \end{bmatrix} \begin{bmatrix} (\beta_1 - \alpha_1)_m \\ (\beta_2 - \alpha_2)_m \\ (\beta_3 - \alpha_3)_m \\ (\beta_4 - \alpha_4)_m \end{bmatrix} \tag{27}$$

The innovation vector is then defined by

$$\nu = \begin{bmatrix} \beta_{om} - \hat{\beta}_o \\ (\beta_I - \alpha_I)_m - (\hat{\beta}_I - \alpha_I) \\ (\beta_{II} - \alpha_{II})_m - (\hat{\beta}_{II} - \alpha_{II}) \\ \beta_{dm} - \hat{\beta}_d \end{bmatrix} \tag{28}$$

The measurement covariance has been assumed given for the computer simulations. It will be updated for each iteration for the state and parameter identifications from transient test results, as explained before.

Numerical Results for Cyclic Pitch Stirring Transients

For the numerical examples presented in the following we assumed as given the product of lift slope and blade solidity ratio $a\sigma = 2\pi/10$, the advance ratio $\mu = .4$, the tip loss factor $B = .97$ and the blade flapping frequency $P = 1.20$. The Lock number is assumed given as $\gamma = 5.0$ for some of the identification runs and assumed unknown in other runs. The control variables θ_I, θ_{II} are assumed given. In previous experience it was found that a moderate noise pollution of the

control variables had no substantial effect on the.
results of the state and parameter identification. For the cases
presented here θ_I and θ_{II} were used in the rotor system equations
without noise pollution. The 4 single blade simulated flapping
angle measurements were polluted with computer generated Gaussian
zero mean noise with a standard deviation of $\sigma_{\beta_k} = .1$. A variety
of values for the pitch stirring acceleration were studied. It was
found that the slower accelerations required a longer time span to
yield the same accuracy of the identified parameters as the faster
accelerations. Here only the case of a cyclic pitch stirring
acceleration of $\dot{\omega} = -.10/\pi$ is presented, using a data length of
12 time units from the start of the transient. Later it was found
that this data length does not provide optimal data utilization and
that for better results a data length of 18 time units should have
been used for $\dot{\omega} = -.10/\pi$.

In preceding studies it was found that better rotor inflow
parameter identification can be achieved for progressing cyclic
pitch stirring as compared to regressive stirring. The reason for
this experience probably is that for regressive stirring the blade
natural frequency is resonance excited and that at the resonance
frequency the dynamic rotor inflow is theoretically zero. All
presented cases are for progressing cyclic pitch stirring accelerations.

It was first attempted to solve the problem in the same way as
described in Chapter 2 of reference 4 by including the initial values
of the flapping angles and of the inflow variables as further unknowns
to be identified. This adds another 7 unknowns in the identification

routine and led to difficulties. It was then decided to use in the
identification algorithm perturbations from the initial conditions
before on-set of cyclic pitch stirring. Thus the initial values for
all state variables are zero and need not be identified.

Fig. 1 shows the cyclic pitch stirring input for a progressing
stirring acceleration of $\dot{\omega} = -.10/\pi$. The amplitude of cyclic pitch
stirring is $\pm 1.5°$. Since the initial value is zero, the maximum
excursion of θ_{II} is from 0 to $-3°$. Fig. 2 shows the flapping
response of blade number 1 with the computer generated noise pollution
corresponding to $\sigma_{\beta_1} = .10$. The polluted values are used in the
state and parameter identification. Five different analytical models
will be discussed here.

(a) Dynamic inflow neglected, Lock number $\gamma = 5$.

(b) Quasistatic dynamic inflow, equivalent Lock number γ^* identified.

(c) Diagonal L-matrix and inflow time constant identified, $\gamma = 5$.

(d) Full L-matrix and inflow time constant identified, $\gamma = 5$.

(e) Full L-matrix and inflow time constant and γ identified.

The inflow model given by Eq. (15) is used. In the following table the
given values (0 or 5), of the parameters are noted. If no value is
given, the parameter is identified.

Model	P_1	P_2	P_3	P_4	P_5	τ	γ
a	0	0	0	0	0	0	5.0
b	0	0	0	0	0	0	
c			0	0			5.0
d							5.0
e							

The results of the parameter identifications based on the analytical models b, c, d, e are given in the following tables:

Model (b), 4.1 CPU sec/Iteration

		γ^*
Initial Estimate		2.50
Iteration	1	3.87
	2	4.08
	3	4.09
$M^{-1/2}$/Ident. Value		.01

Model (c), 9.7 CPU sec/Iteration

		P_1	P_2	P_5	τ
Initial Estimate		.90	1.08	.88	1.08
Iteration	1	.26	.55	-.13	.38
	2	.36	.62	.11	.53
	3	.49	.85	.30	.68
	4	.54	.95	.36	.74
	5	.54	.96	.37	.74
$M^{-1/2}$/Iden. Value		.30	.17	.19	.12

Model (d), 13.3 CPU sec/Iteration

		P_1	P_2	P_3	P_4	P_5	τ
True Value		1.00	1.20	-.40	.40	.80	1.20
Initial Estimate		.90	1.08	-.44	.36	.88	1.08
Iteration	1	.74	.74	-.71	.16	.61	1.09
	2	.83	.90	-.72	.29	.76	1.19
	3	.81	.86	-.68	.25	.74	1.16
	4	.81	.87	-.69	.26	.75	1.16
	5	.81	.87	-.69	.26	.75	1.16
$M^{-1/2}$/Iden. Value		.57	.63	.70	1.98	.77	.51

Model (e), 16 CPU sec/Iteration

	P_1	P_2	P_3	P_4	P_5	τ	γ
True Value	1.00	1.20	-.40	.40	.80	1.20	5.00
Initial Estimate	.90	1.08	-.44	.36	.88	1.08	4.00
Iteration 1	1.01	.63	-.89	.35	.59	1.05	4.85
2	.86	.95	-.85	.38	.81	1.22	4.96
3	.79	.81	-.66	.23	.70	1.10	4.97
4	.82	.87	-.71	.27	.75	1.17	4.99
5	.81	.85	-.70	.27	.74	1.14	4.98
$M^{-1/2}$/Iden. Value	.60	.76	.76	2.06	.86	.67	.08

For models (b) and (c) no true values of the unknown parameters are
available, since these models are different from that which generated
the simulated measurements. For models (d) and (e) the true
parameter values are known. One cannot expect that P_1 P_2 P_3 τ for
Model (c) are the same as for Model (d) or (e). Apparently the much
lower value for τ in Model (c) has to make up for the omission of
the off-diagonal terms in the L-matrix. The parameters of Models (d)
and (e) are almost the same. Thus identification of γ does not affect
the accuracy of the other parameters, but it does increase the CPU
time per iteration from 13.3 to 16 seconds. The relative parameter
standard deviations $M^{-1/2}$/Ident. Value are rather large, indicating
that not sufficient data length has been used. We will see later
that a substantial reduction in $M^{-1/2}$ is possible for greater data
length.

Verification by Response Comparisons

The identified models have first been verified by comparing the responses for the transients used in the identification. The comparison in Fig. 3 is between the exact responses - solid lines in Fig. 3 and subsequent figures - with the response from the identified model - dot lines in Fig. 3 and subsequent figures-. Fig. 3a is for Model (a) without rotor inflow using the cyclic pitch stirring acceleration $\dot{\omega}$ = -.10/π. It is seen that substantial errors of Model (a) occur in the β_I response, smaller errors in the β_O response and insignificant errors in the β_d and β_{II} responses. These errors are the basis for the inflow parameter identifications.

Fig. 3b is for Model (b) using the equivalent Lock number concept. The errors in the β_O and β_d responses are now insignificant, while the β_I and β_{II} responses show relatively small errors. Thus the equivalent Lock number concept appears to be quite useful for this case.

Fig. 3(c) is for Model (c) with given Lock number and 4 identified inflow parameters; the diagonal L-matrix and one time constant. All 4 response variables show negligible errors. Figs. 3(d) and 3(e) are for Models (d) and (e). Though more inflow parameters have been used, the response errors are noticeable though still very small. One can then conclude that Model (b) identifying only γ^* and using 4.1 CPU seconds per iteration may be adequate in some cases, that Model (c) identifying 4 inflow parameters and using 9.7 CPU seconds per iteration is excellent, and that the inclusion of the off-diagonal terms in the L-matrix is not necessary in this particular case. A sixth model not

considered here would probably be useful in state and parameter
identifications from test transients, namely Model (c) including
γ as unknown parameter. The Lock number was found in all cases
easy to identify accurately. Theoretical values for γ are not
always reliable since they involve the blade elastic mode shape,
the lift slc_e and the exact blade mass distribution.

The next step in the verification of the identified models is
to compare responses in transients that have not been used for the
parameter identification. Figs. 4 and 5 show the true responses to
a collective and to a longitudinal cyclic unit step input respectively
as compared to the responses of Models (a), (b) and (e). Again Model
(b) is a substantial improvement over Model (a) that omits rotor
dynamic inflow effects. Model (e) gives almost the correct responses.
Presumably Model (c) with or without identification of γ would show
the same excellent agreement with the assumed "true" model. Though
the inflow parameters P_1 to P_5 and τ in the various models deviate
to a certain extent from the true values, the responses predicted
by Models (c), (d), (e) are in very good agreement with the responses
of the true model not only for the cyclic pitch stirring transient
but also for quite different transients.

Inflow Model with Three Time Constants

Particularly at high advance ratio the time constants for pitch
and roll could be different, since different participating air masses
might be anticipated. It, therefore, appeared of interest to study a
case where 3 instead of 1 time constant are assumed to be unknown.
This is a further extension of Model (e). The complete L-matrix in

addition to γ was identified. The parameters were defined somewhat differently from Eq. (15), namely by

$$\begin{bmatrix} \dot{v}_O \\ \dot{v}_I \\ \dot{v}_{II} \end{bmatrix} + \mu \begin{bmatrix} \tau_O & 0 & 0 \\ 0 & \tau_I & 0 \\ 0 & 0 & \tau_{II} \end{bmatrix} \begin{bmatrix} L_{11} & 0 & 0 \\ 0 & L_{22} & L_{23} \\ 0 & L_{32} & L_{33} \end{bmatrix} \begin{bmatrix} v_O \\ v_I \\ v_{II} \end{bmatrix} = \begin{bmatrix} \tau_O & 0 & 0 \\ 0 & \tau_I & 0 \\ 0 & 0 & \tau_{II} \end{bmatrix} \begin{bmatrix} c_T \\ -c_M \\ -c_L \end{bmatrix}$$

(29)

The following table gives the results of 3 iterations. The value of the criterion function

$$J = \sum_{i=1}^{N} (Y_{im} - \hat{Y}_i)^T R^{-1} (Y_{im} - \hat{Y}_i)$$

(30)

is given in the last column. Contrary to the preceding cases the assumed measurement standard deviation for all simulated measured variables is $\sigma = .05$, ($R^{-1} = 400\,I$) instead of $\sigma = .1$, and the time used for the identification is 18 instead of 12. Same as before the rotor advance ratio is $\mu = .4$, and the cyclic pitch stirring acceleration is $\dot{\omega} = -.1/\pi$, taken in the progressing sense. Also, same as before, the time interval for the numerical integrations is .1.

Model (e) with 3 Time Constants, 45 CPU sec/Iteration

	L_{11}	L_{22}	L_{23}	L_{32}	L_{33}	τ_O	τ_I	τ_{II}	γ	J
True Value	1.00	.42	-.17	.08	.17	1.18	8.8	8.8	3.2	
Initial Est.	.83	.33	-.14	.06	.14	1.35	7.0	7.0	4.5	8720
Iteration 1	1.16	.29	-.06	.08	.16	1.15	3.8	8.1	3.1	951
2	.97	.35	-.12	.06	.18	1.42	4.6	8.5	3.2	716
3	1.00	.37	-.11	.06	.17	1.43	4.8	8.5	3.2	
Error/True Value	0	.12	.35	.25	0	.21	.45	.03	0	
$M^{-1/2}$/Ident. Value	.12	.08	.71	.18	.11	.13	.42	.10	.01	

In comparison to the case for Model (e) with one time constant there is better convergence and there are smaller parameter errors. The relative predicted parameter error ($M^{-1/2}$/Identified Value) shows the same trend as the actual relative error, γ having the best and L_{23} and τ_I the worst accuracy. The predicted parameter errors are much smaller than for the case of Model (e) presumably because of the smaller simulated measurement error (σ = .05 instead of .1) and the longer data length (t = 1J instead of 12). The CPU time per iteration is almost 3 times the value for Model (e) with one time constant. In all the cases presented here the initial estimates are not drastically different from the true values of the parameters. It was found that very much larger errors in the initial estimates can be tolerated without affecting the quality of the convergence or of the final estimates.

A somewhat different presentation for verifying the identified model is given for this case as compared to the preceding cases. In Figs. 6a to 6d the blade flapping response computed with the identified model (solid lines) is compared to the simulated measurements (crosses). The good fit of the analytical model is evident. Figs. 7a to 7c show the dynamic inflow variables ν_o, ν_I, ν_{II} computed with the identified model. Particularly ν_{II} shows very substantial fluctuations.

Optimum Data Utilization

In reference 4 Chapter 3 a differential equation for the inverted information matrix M^{-1} is developed that allows to compute the Cramér-Rao lower bound for the parameter covariances vs. the duration of the transient used in the parameter identification process. For the

example given in reference 4 it was found that there exists an optimum data length beyond which no improvement in the parameter errors can be expected. It is of interest to find out whether or not such an optimum data length can also be defined for the much more complex cases studied in this report.

The case presented here refers to Model (e) with one time constant, the dynamic rotor inflow being represented by Eqs. (13) and (15). The advance ratio is again $\mu = .4$. The simulated measurement standard deviation is $\sigma = .05$. The transient is a progressing cyclic pitch stirring excitation with an acceleration $\dot{\omega} = -.1/\pi$. The true Lock number is $\gamma = 5$. Fig. 8 shows the predicted parameter standard deviations (Cramér-Rao lower bounds) divided by the parameter values vs. the duration of the transient used in the identification process. The Lock number γ shows the lowest relative error, the parameter P_1 ultimately the highest. It is remarkable that all 7 parameters reach their asymptotic relative error at about the same $t = 18$. Thus using a transient time of $t = 12$ as was done here for the identification of Model (e) with one time constant (but not of Model (e) with three time constants), does not give optimal data utilization. On the other hand Fig. 8 shows that extending the data length used for the parameter identifications much beyond $t = 18$ would be wasteful of computer time and would not result in better accuracies of the parameter estimates.

Numerical Results for Hub Stirring Transients

As an alternative to cyclic pitch stirring transients hub stirring transients have been considered, and the rotor equations for this case have been presented (Eqs. (23) to (28)). The question is whether the accuracy of the parameter identifications is affected when using hub stirring instead of cyclic pitch stirring. For blades articulated at the rotor center cyclic pitch stirring and hub stirring are identical and lead to identical flapping responses. For rotors with off-set hinges or for hingeless rotors there are, however, differences in the two modes of transient excitation.

Model (e) with one time constant and the rotor inflow defined by Eqs. (13) and (15) has been assumed for the study. The advance ratio is $\mu = .4$. The stirring acceleration is $\dot{\omega} = -.1/\pi$ in the progressing sense. Contrary to the preceding analysis for Model (e) the time step has been increased from $\Delta t = .1$ to .2. The duration of the transient has also been increased from $t = 12$ to 24 so that the computer time remains the same.

Model (e), Hub Stirring, $\Delta t = .2$, $t = 24$, 16 CPU sec/Iteration

		P_1	P_2	P_3	P_4	P_5	τ	γ
True Value		1.00	1.20	-.40	.40	.80	1.20	5.00
Initial Estimate		.50	.60	-.20	.20	.40	1.80	4.00
Iteration	1	1.14	.57	-.50	.50	.60	1.11	4.81
	2	.94	1.04	-.65	.60	.82	1.37	5.03
	3	.90	1.17	-.59	.40	.81	1.35	5.06
	4	.88	1.15	-.56	.33	.78	1.32	5.06
	5	.88	1.16	-.56	.33	.78	1.32	5.06
$M^{-1/2}$/Ident. Value		.25	.26	.30	.75	.24	.18	.02

To compare with the equivalent cyclic pitch stirring case, an analysis of this case was made on the same basis, that is using a time step $\Delta t = .2$ and a duration $t = 24$.

Model (e), Cyclic Pitch Stirring, $\Delta t = .2$, $t = 24$, 16 CPU sec/Iteration

		P_1	P_2	P_3	P_4	P_5	τ	γ
True Value		1.00	1.20	-.40	.40	.80	1.20	5.00
Initial Estimate		.50	.60	-.20	.20	.40	1.80	4.00
Iteration	1	.96	.91	-.43	.44	.68	.94	4.77
	2	.72	1.26	-.46	.40	.86	1.16	4.96
	3	.75	1.26	-.42	.34	.84	1.16	4.97
	4	.75	1.26	-.42	.34	.84	1.17	4.98
	5	.75	1.26	-.42	.34	.84	1.17	4.98
$M^{-1/2}$/Ident. Value		.27	.16	.27	.27	.22	.26	.04

Note that in both cases the errors in the initial estimates are much larger than in the preceding cases, yet good convergence is obtained. In comparing the hub stirring with the cyclic pitch stirring case, there are only insignificant differences in the parameter errors and in the rates of conversion. The predicted parameter errors are also rather close except for a larger predicted error for P_4 in the case of hub stirring. In both cases the predicted and actual errors for the Lock number γ are quite small. In comparison to the previous analysis for Model (e) with one time constant and $\Delta t = .1$, $t = 12$, both the predicted and actual parameter errors are much smaller despite identical computer CPU time.

Conclusions

Rotor state and parameter identifications at .4 rotor advance ratio
have been performed based on simulated blade flapping measurements for
an analytical rotor model that assumes straight blades flexibly hinged
at the rotor center. Reversed flow, stall and compressibility effects
were omitted, but periodic coefficients in the equations of motion for
forward flight conditions were retained. All state and parameter
identifications were performed with brief periods of accelerated cyclic
pitch or hub stirring. The following conclusions can be drawn from the
study.

1. The maximum likelihood method with a fixed error covariance matrix
   is well suited for the problem and gives good convergence in all
   cases.

2. Using a model with an identified equivalent Lock number substantially
   improves the predicted flapping responses in comparison to those
   with neglected rotor dynamic inflow, but still leaves some errors in
   the responses.

3. An identified dynamic rotor inflow model with 4 parameters that
   include one time constant gives almost perfect response predictions.

4. The addition of 4 more inflow parameters including 2 further time
   constants and of the Lock number does not affect the rate of
   convergence or the accuracy of the estimates, though it requires
   much more computer CPU time per iteration.

5. Cyclic pitch stirring and hub stirring transients are equally
   suitable for the parameter identifications.

6. The accuracies with which the various parameters can be identified are quite different from each other, the Lock number having the highest accuracy. Despite unavoidable inaccuracies in some of the parameters, even relatively large errors in such parameters have little effect on the responses.

7. There is a clearly defined optimal data length that can be computed. More data do not bring improved accuracy of the estimates, while a shorter data length leads to rapidly increasing errors in the estimates.

8. The time step used for the numerical integrations is not a critical quantity. Both $\Delta t = .1$ and $.2$ appear to be satisfactory.

References

1. Hohenemser, K. H. and Yin, S. K., "Methods Studies Toward Simplified Rotor-Body Dynamics", Part I of First Yearly Report under Contract NAS2-7613, June 1974.

2. Hohenemser, K. H. and Yin, S. K., "Computer Experiments in Preparation of System Identification from Transient Rotor Model Tests", Part II of First Yearly Report under Contract NAS2-7613, June 1974.

3. Hohenemser, K. H. and Crews, S. T., "Experiments with a Four-Bladed Cyclic Pitch Stirring Model Rotor", Part III of First Yearly Report under Contract NAS2-7613, June 1974.

4. Hohenemser, K. H., Banerjee, D., and Yin, S. K., "Methods Studies on System Identification From Transient Rotor Tests", Part I of Second Yearly Report under Contract NAS2-7613, June 1975.

5. Hohenemser, K. H. and Crews, S. T., "Additional Experiments with a Four-Bladed Cyclic Pitch Stirring Model Rotor". Part II of Second Yearly Report under Contract NAS2-7613, June 1975.

6. Hohenemser, K. H., Banerjee, D., and Yin, S. K., "Rotor Dynamic State and Parameter Identification From Simulated Forward Flight Transients", Part I of Third Yearly Report under Contract NAS2-7613, June 1976.

7. Hohenemser, K. H. and Crews, S. T., "Rotor Dynamic State and Parameter Identification From Hovering Transients", Part II of Third Yearly Report under Contract NAS2-7613, June 1976.

8. Hohenemser, K. H. and Yin, S. K., "On the Use of First Order Rotor Dynamics in Multiblade Coordinates", 30th Annual National Forum of the American Helicopter Society, May 1974, Preprint No. 831.

9. Ormiston, R. A. and Peters, D. A., "Hingeless Rotor Response with Non-Uniform Inflow and Elastic Blade Bending", J. of Aircraft, Vol. 9, No. 10, Oct. 1972, pp. 730-736.

10. Peters, D. A., "Hingeless Rotor Frequency Response with Unsteady Inflow", Rotorcraft Dynamics, NASA SP 352, February 1974.

11. Hohenemser, K. H. and Yin, S. K., "Some Applications of the Method of Multiblade Coordinates", J. American Helicopter Soc., Vol. 17, No. 3, July 1972.

Figure Captions

Fig. 1   Cyclic Pitch Stirring Inputs with Zero Initial Values for
Progressing Stirring Acceleration $\dot{\omega} = -.10/\pi$.

Fig. 2   Single Blade Flapping Response with Simulated Measurement
Errors, $\sigma_{\beta_k} = .1$.

Fig. 3   Cyclic Pitch Stirring Response Comparisons.

Fig. 4   Response Comparisons for Collective Pitch Unit Step Input.

Fig. 5   Response Comparisons for Longitudinal Cyclic Pitch Unit Step
Input.

Fig. 6   Identified Flapping Responses Using 3 Time Constants.

Fig. 7   Identified Rotor Dynamic Inflow Using 3 Time Constants.

Fig. 8   Relative Parameter Standard Deviation vs. Duration of Transient.
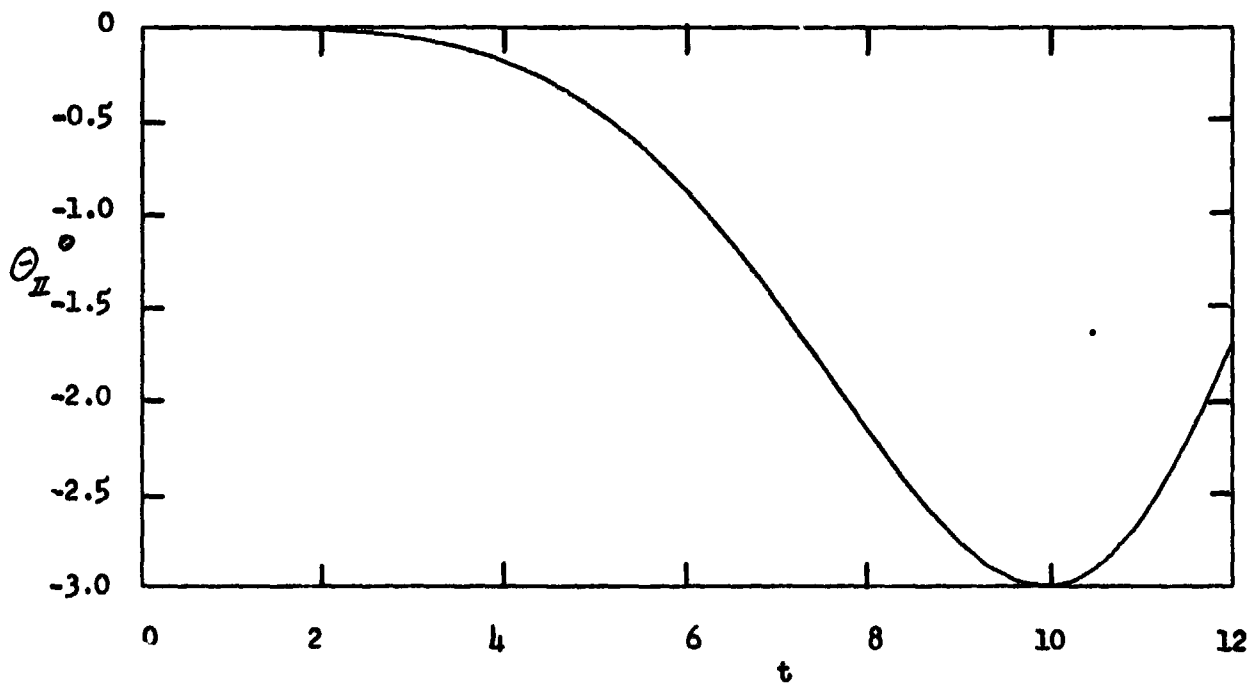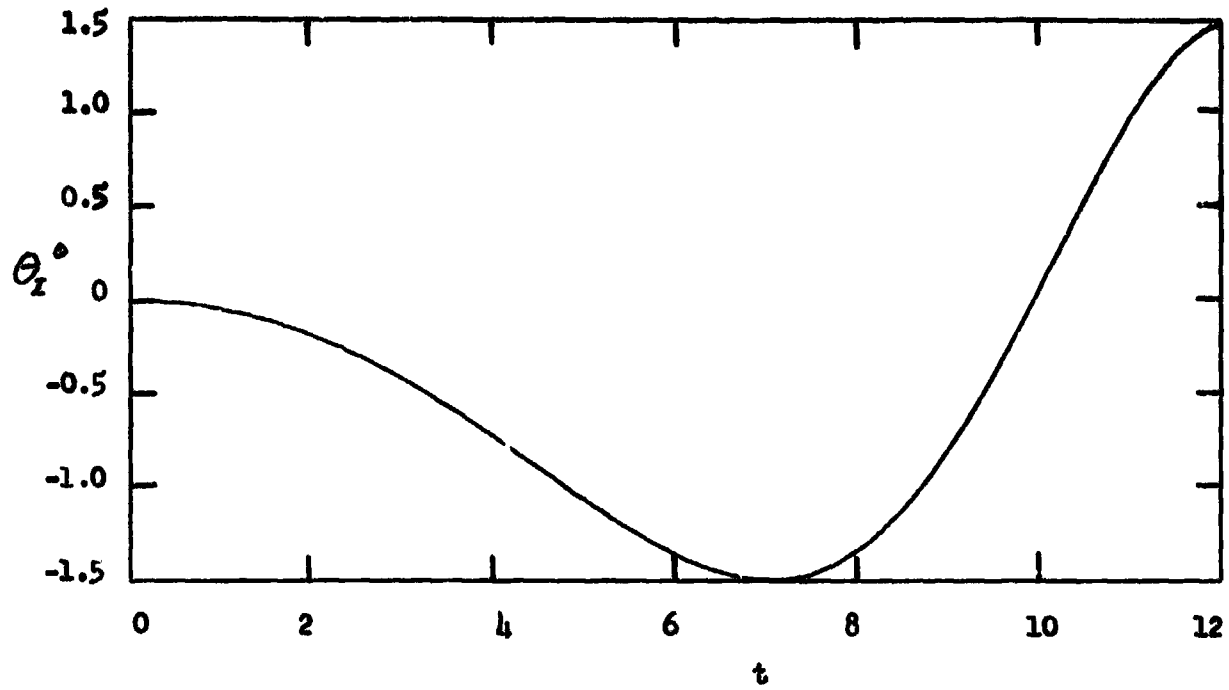
Fig. 1
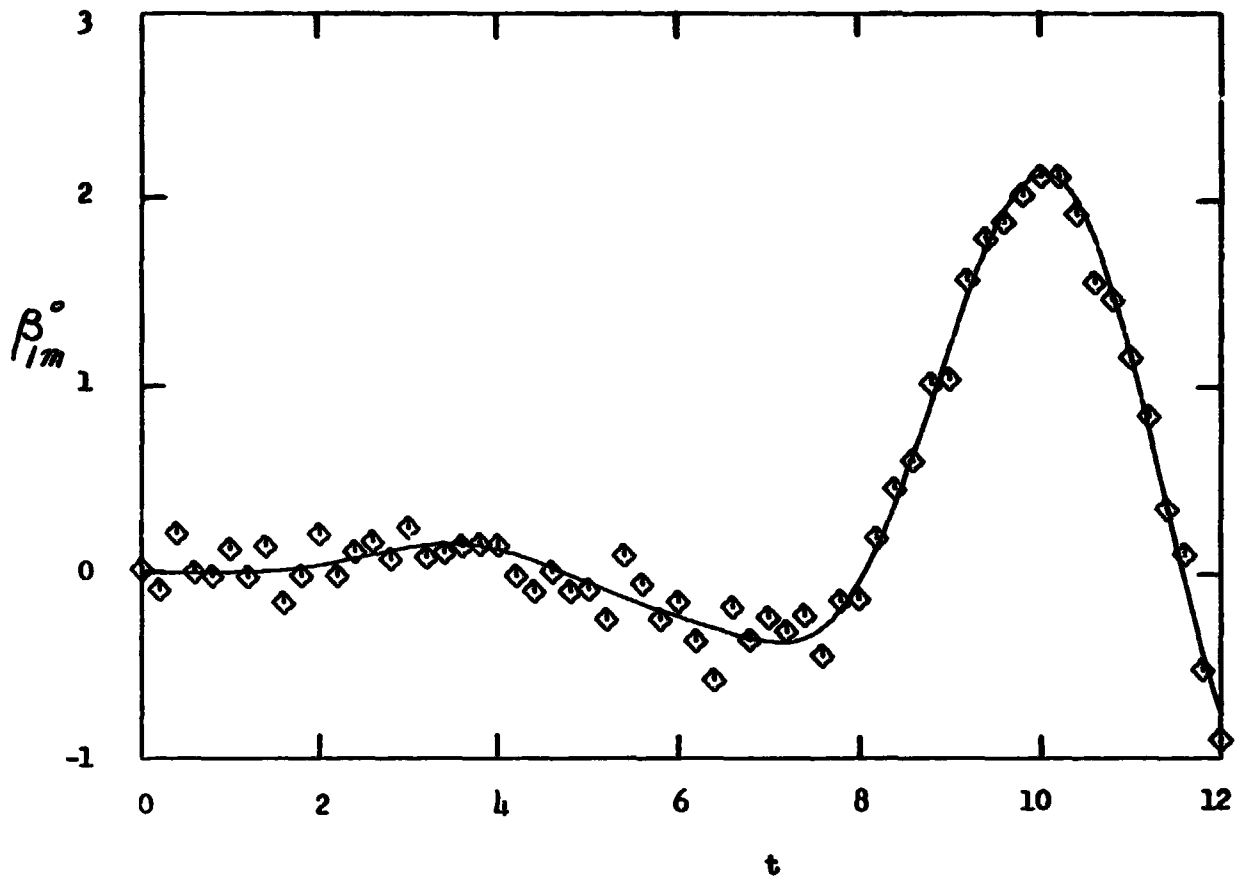
Fig. 2
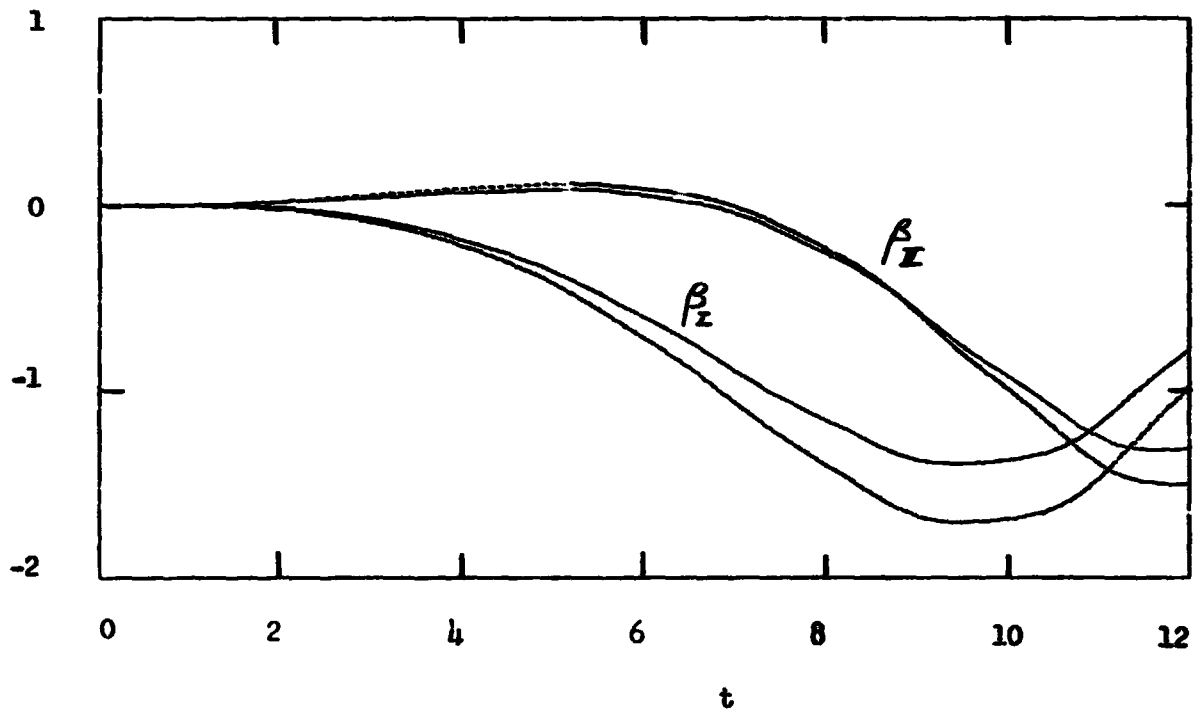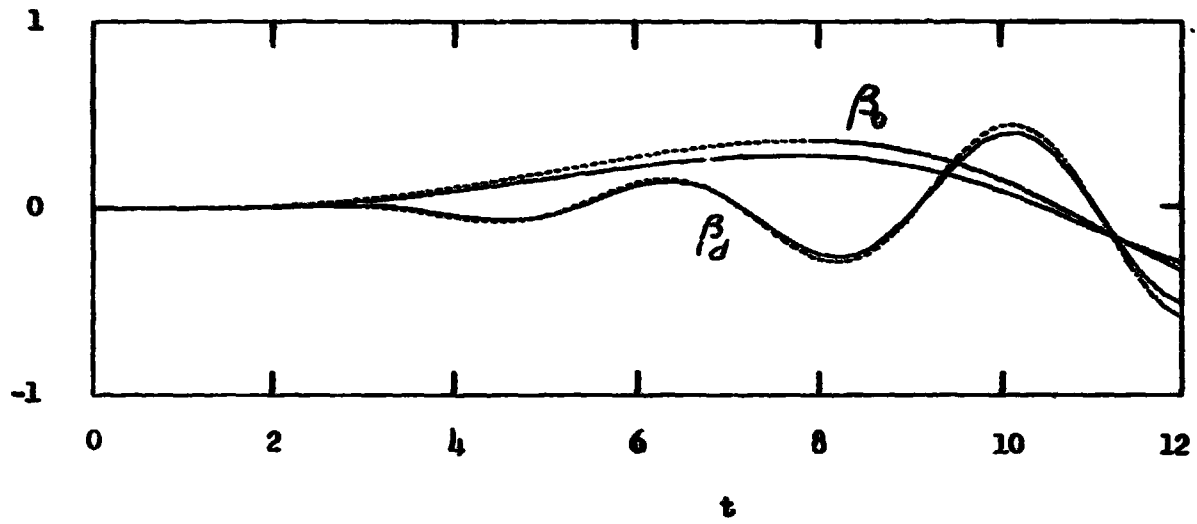
Fig. 3a, Model (a)
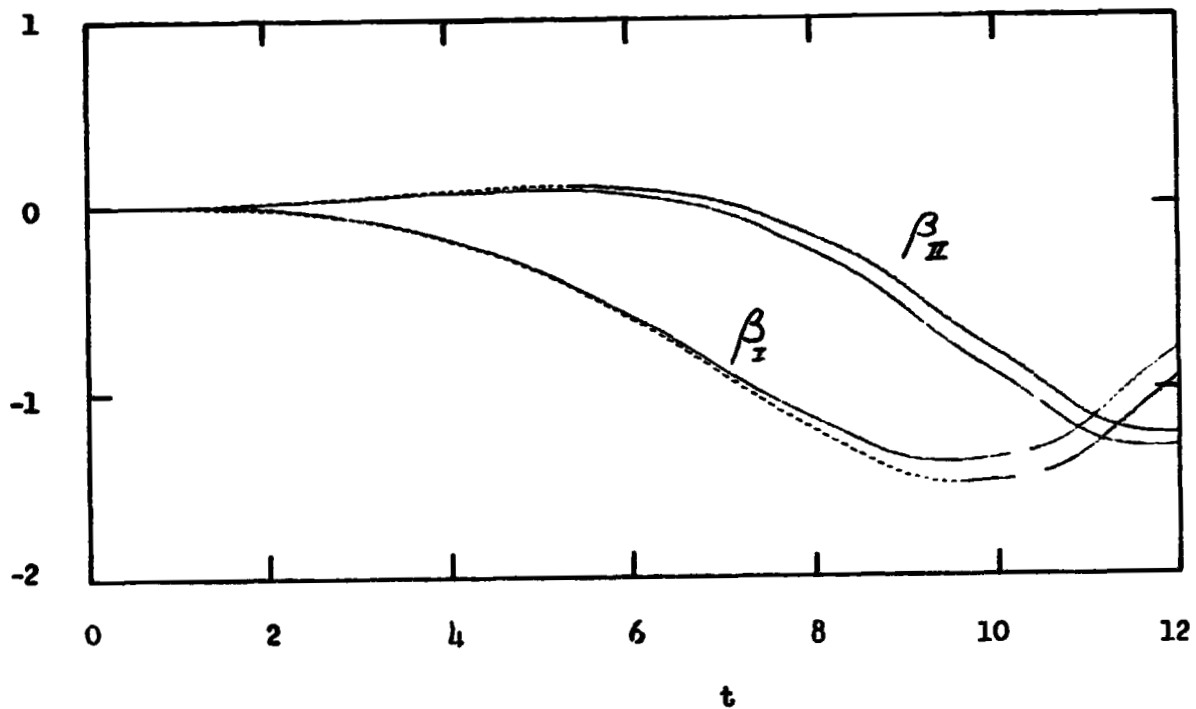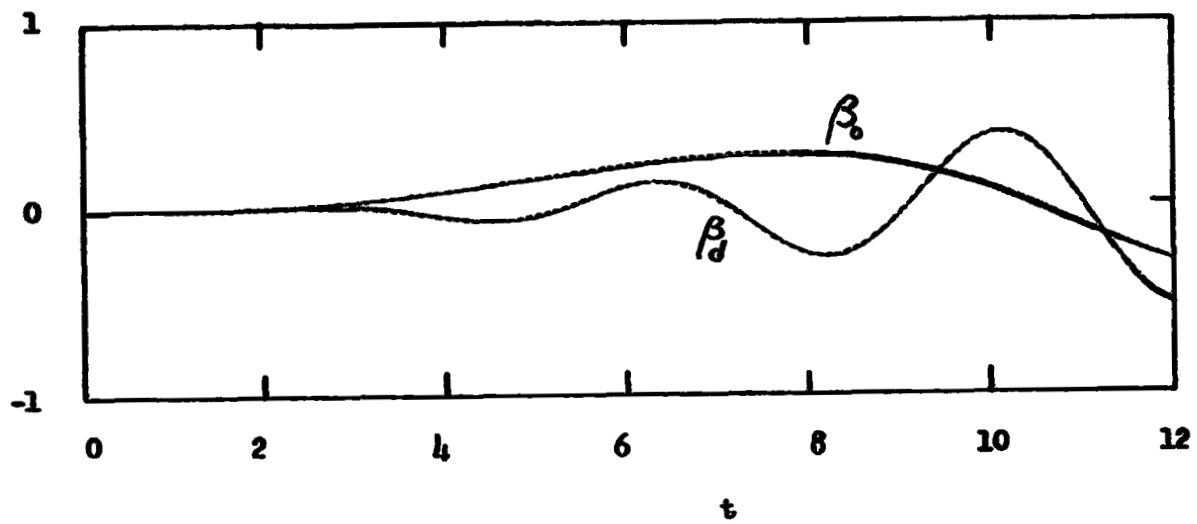
Fig. 3b, Model (b)
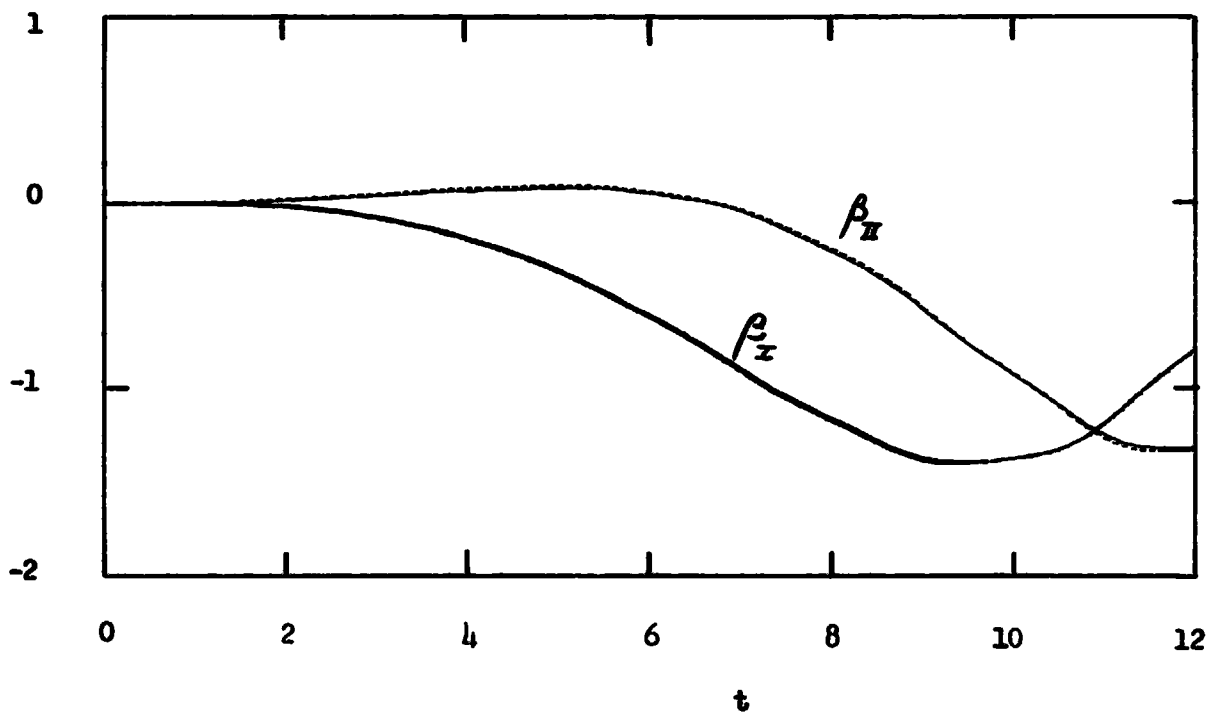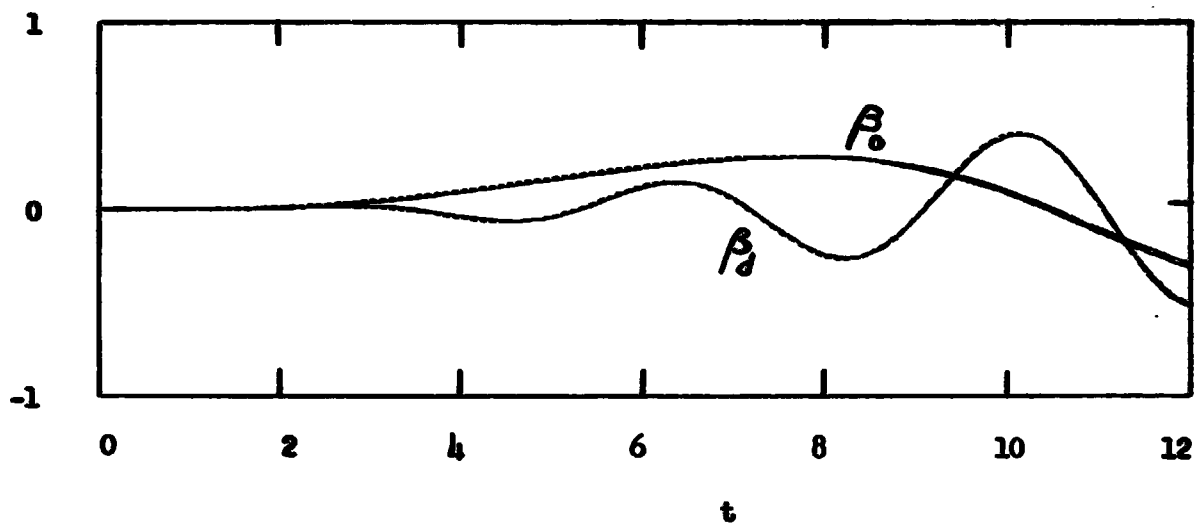
Fig. 3c, Model (c)
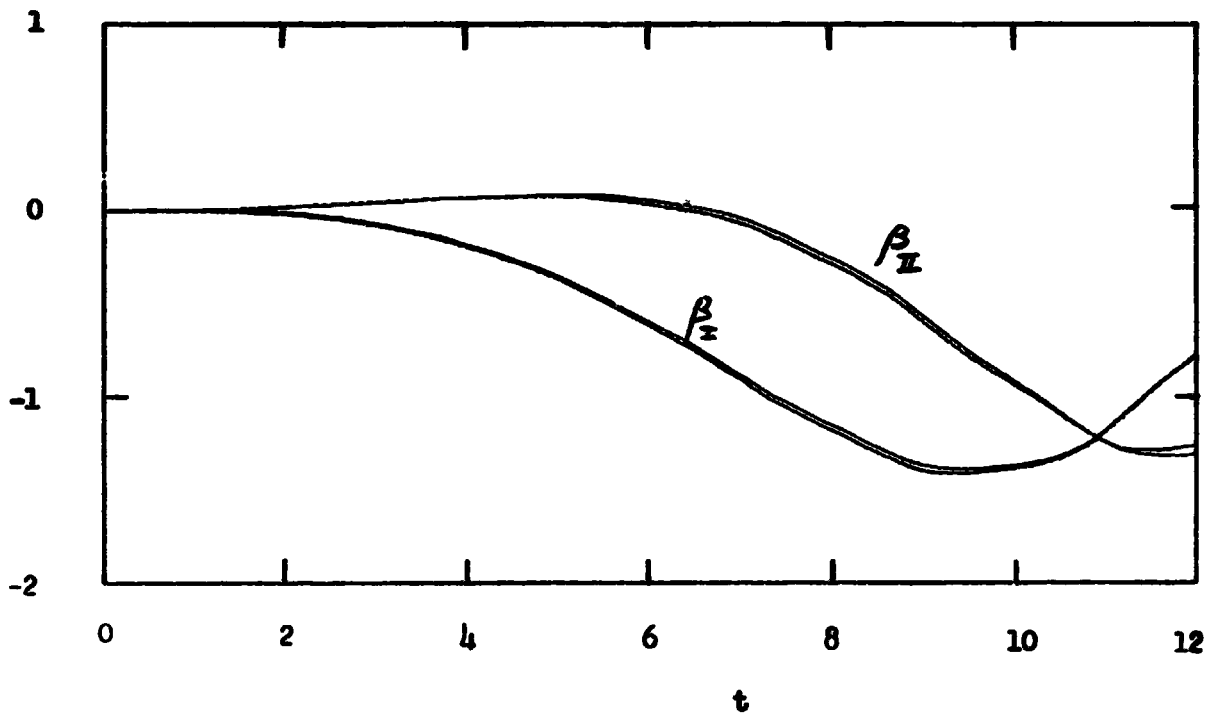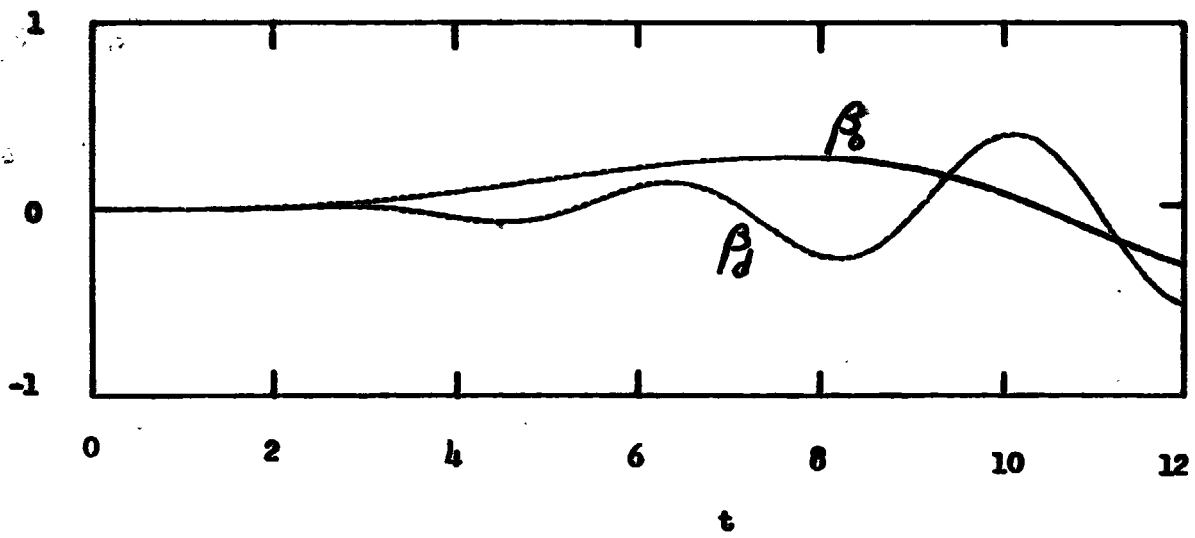
Fig. 3d, Model (d)
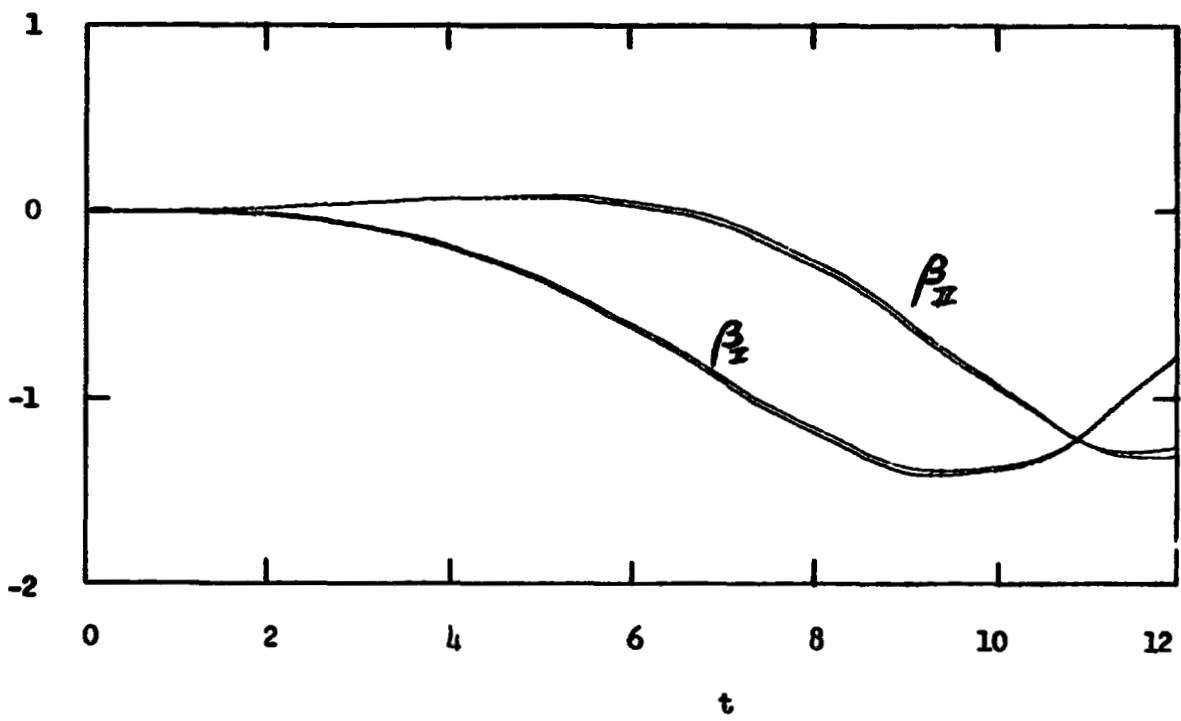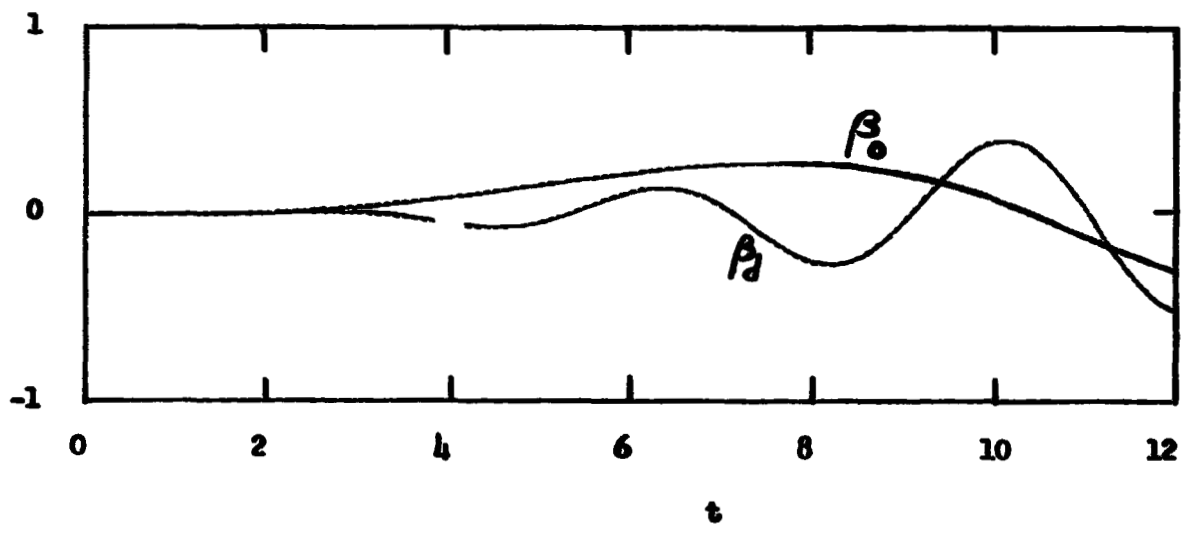
Fig. 3e, Model (e)
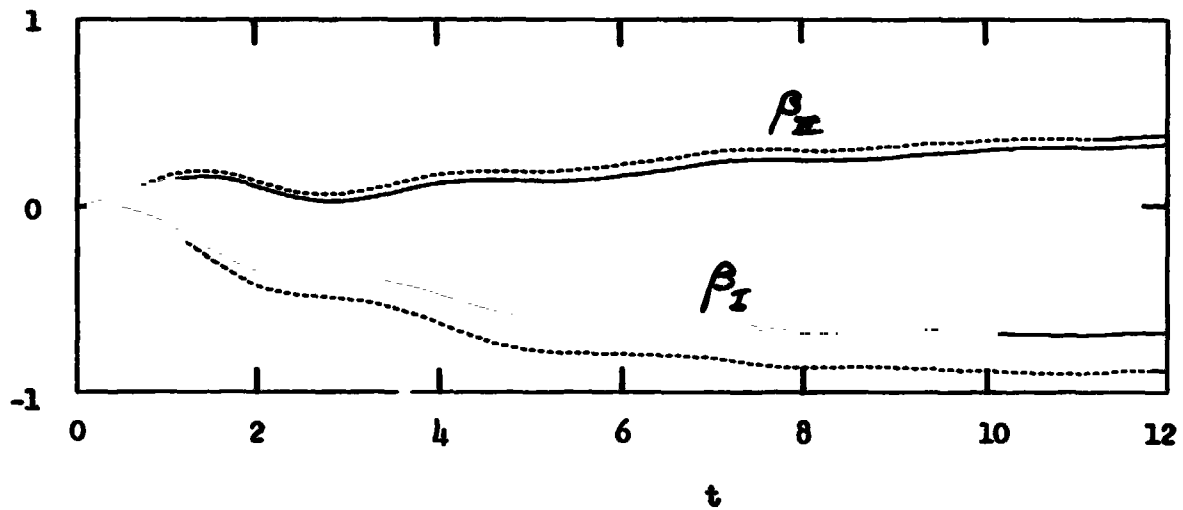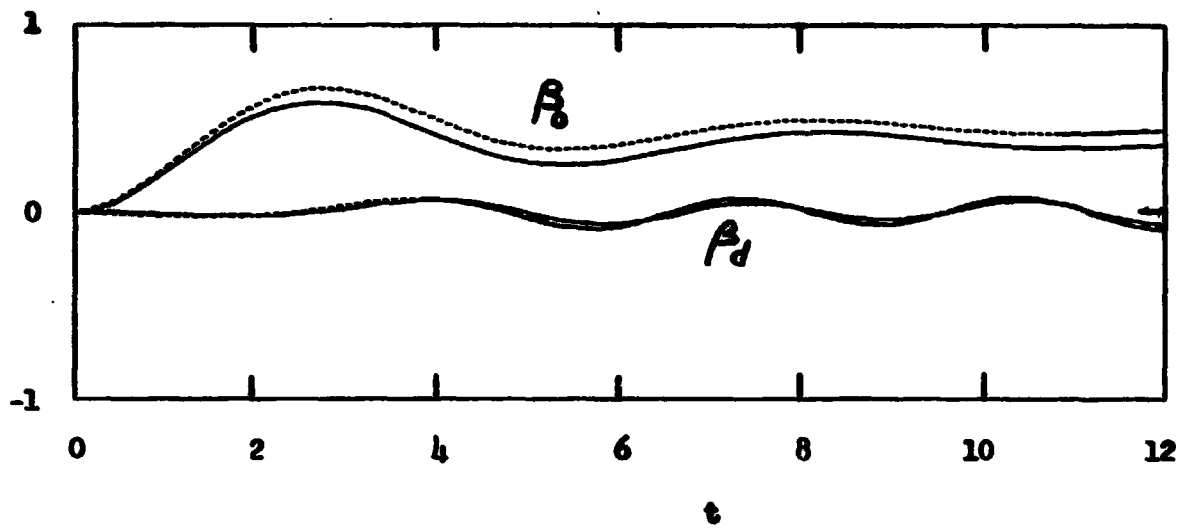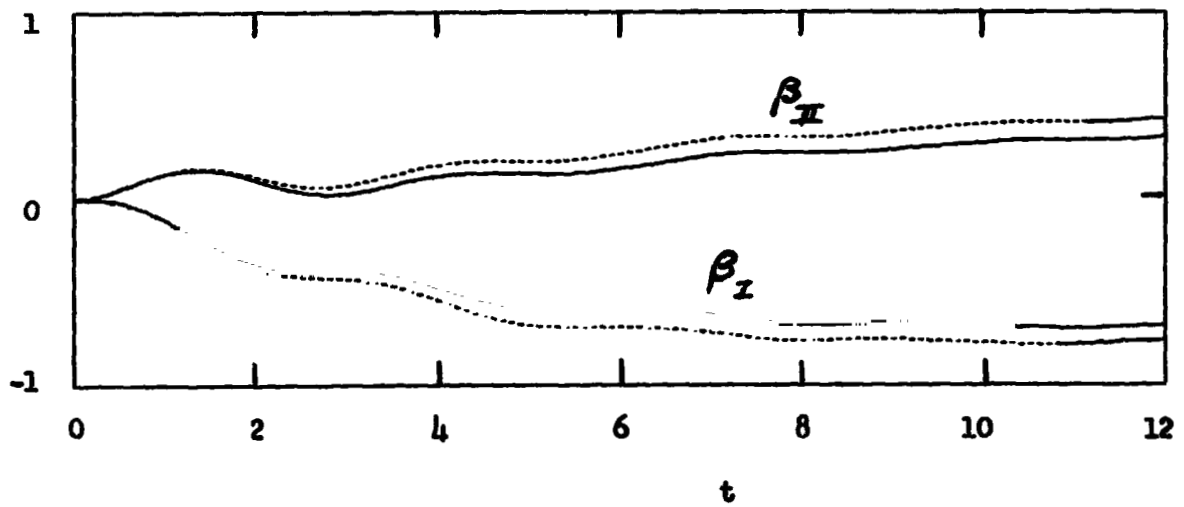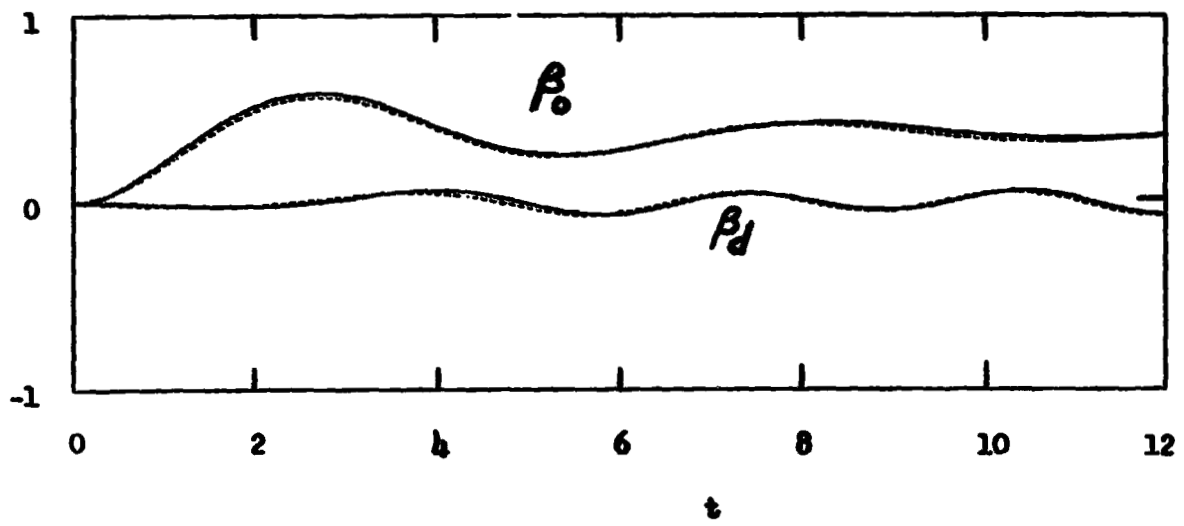
Fig. 4a, $\theta_0 = u(t)$, Model (a)

Fig. 4b, $\theta_0 = u(t)$, Model (b)
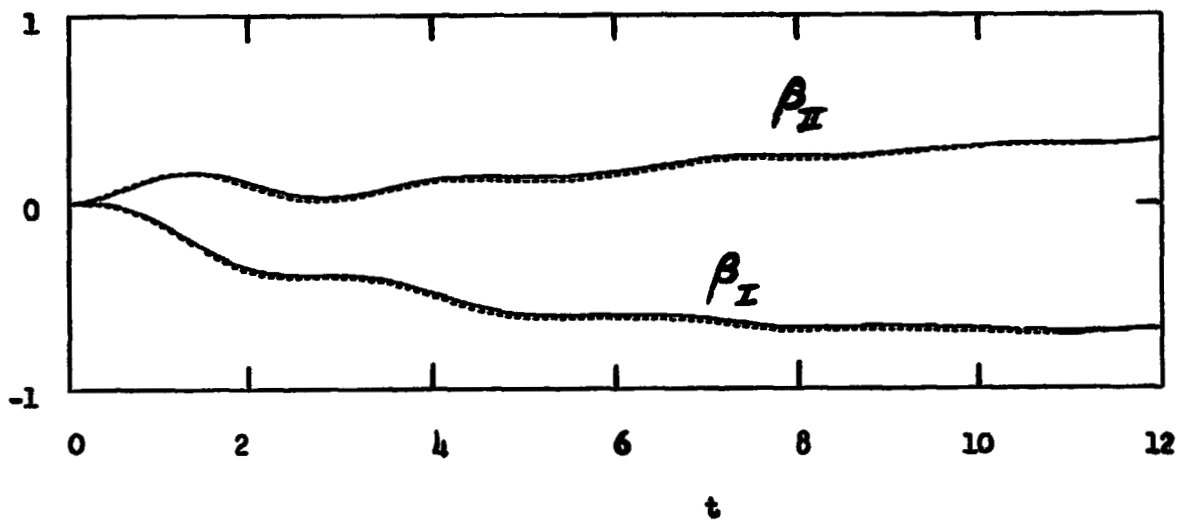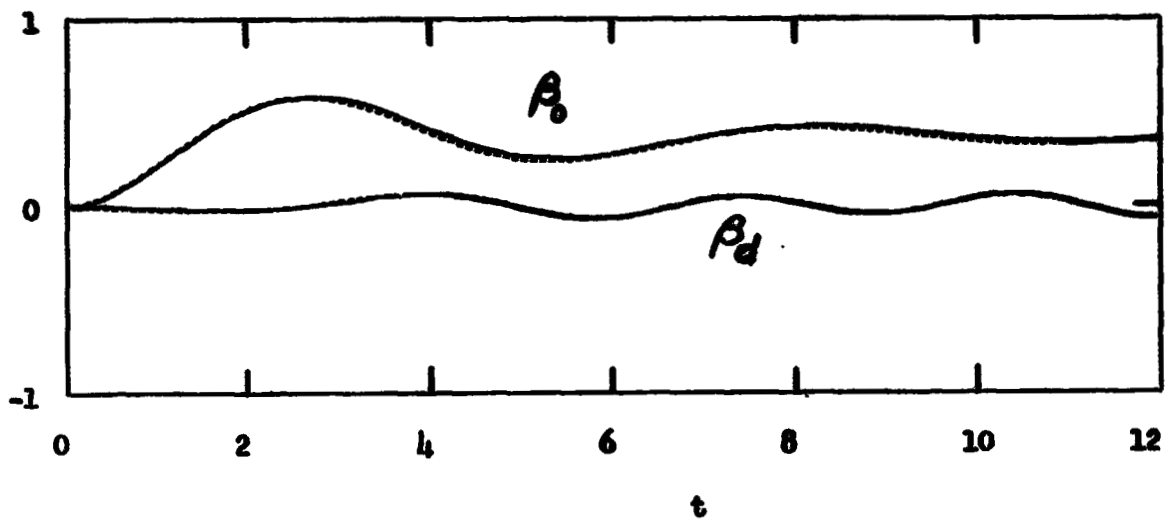
Fig. 4c, $\theta_O = u(t)$, Model (e)
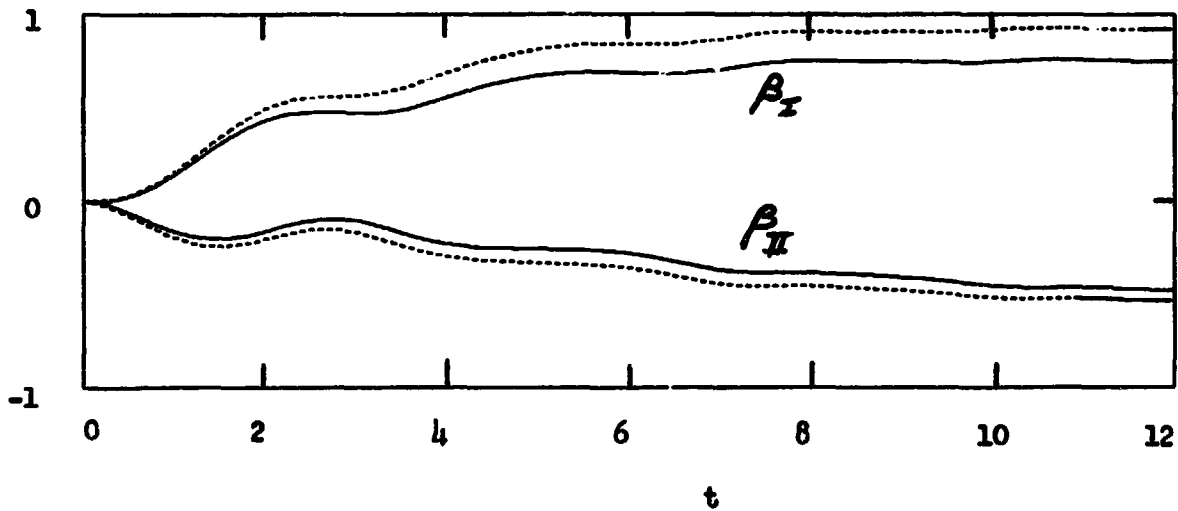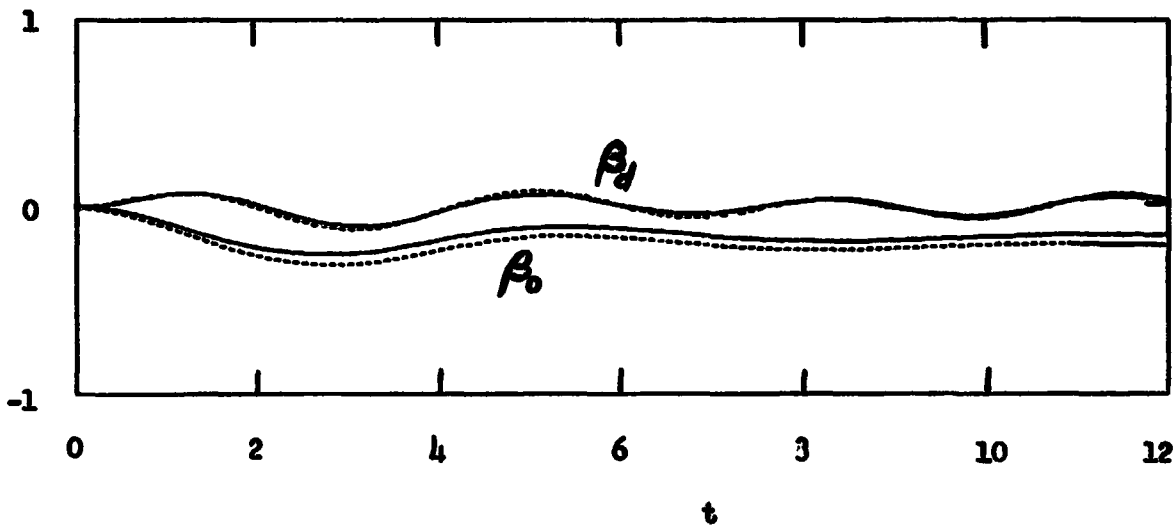
Fig. 5a, $\theta_I = u(t)$, Model (a)
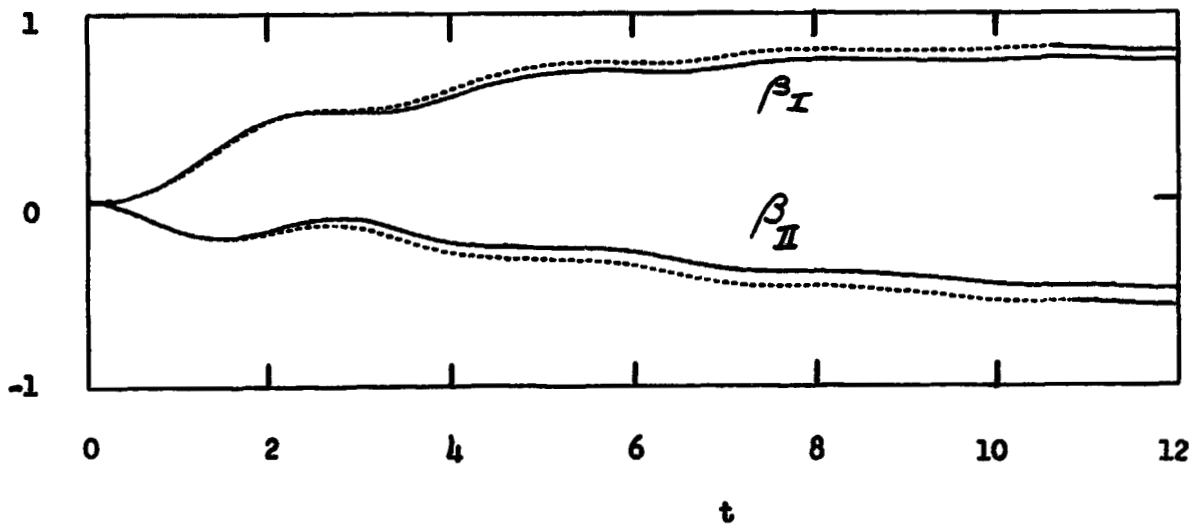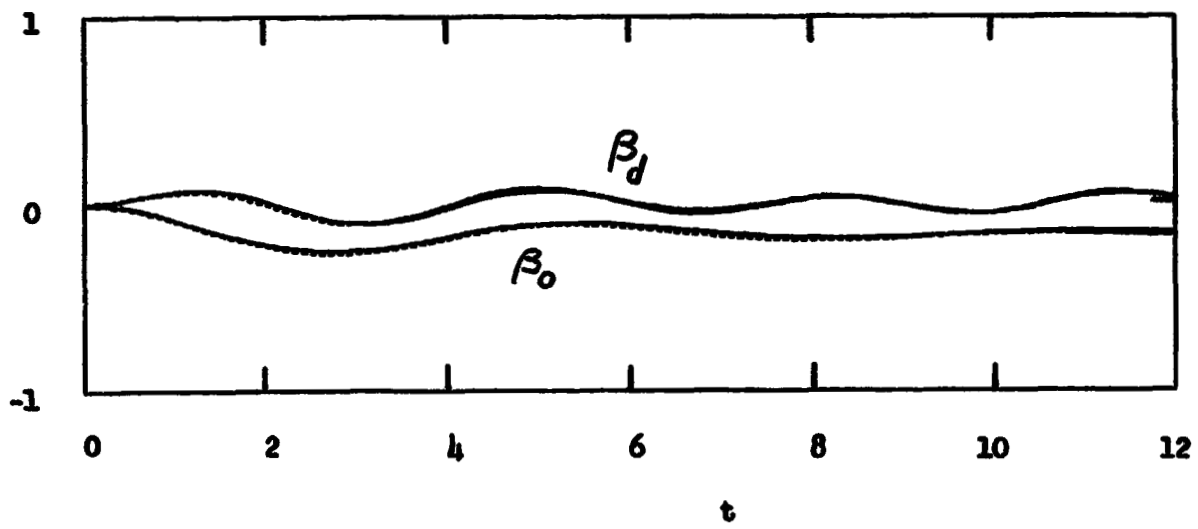
Fig. 5b, $\theta_I = u(t)$, Model (b)
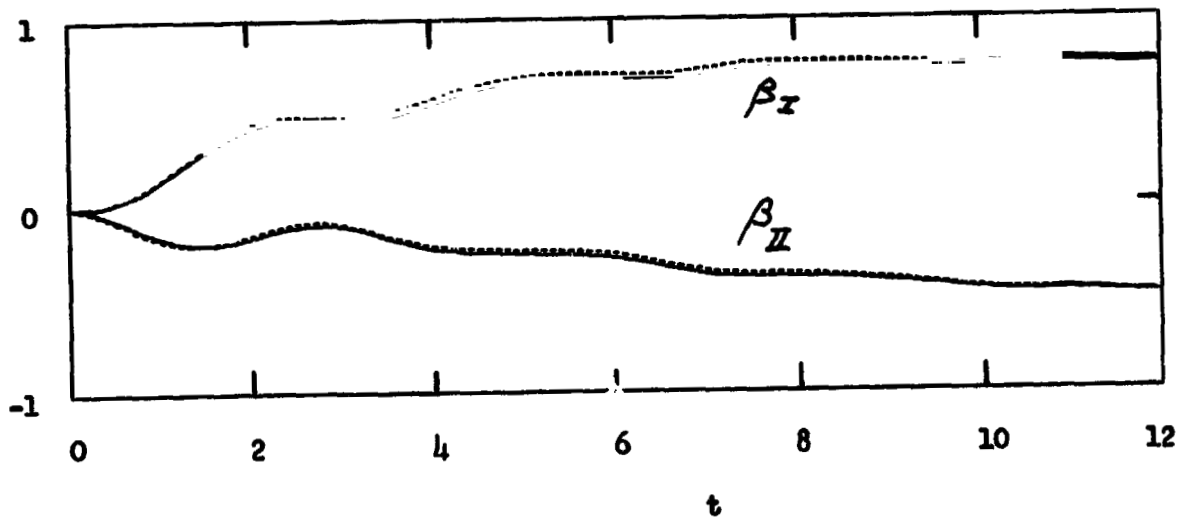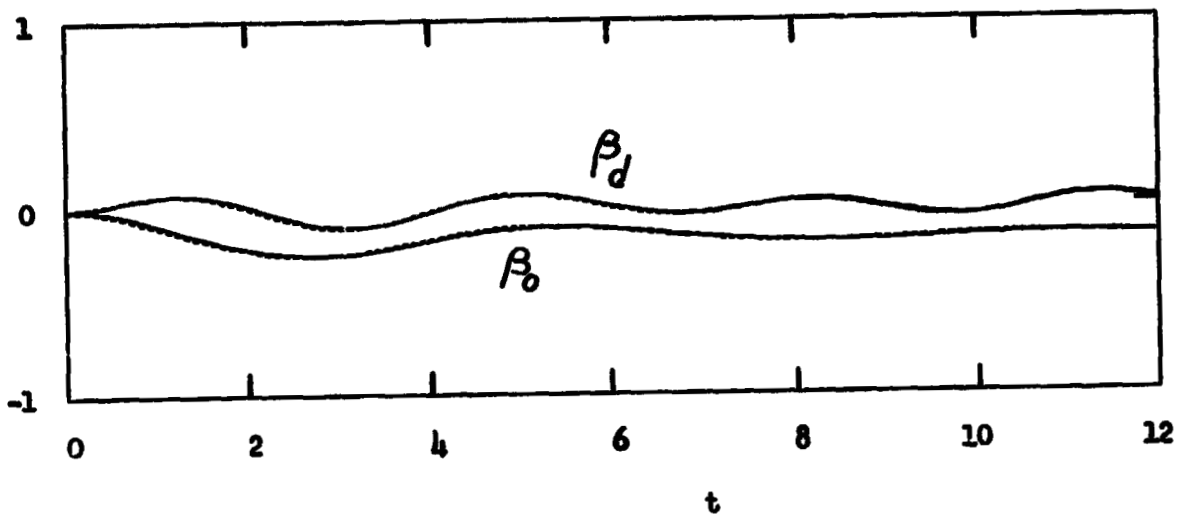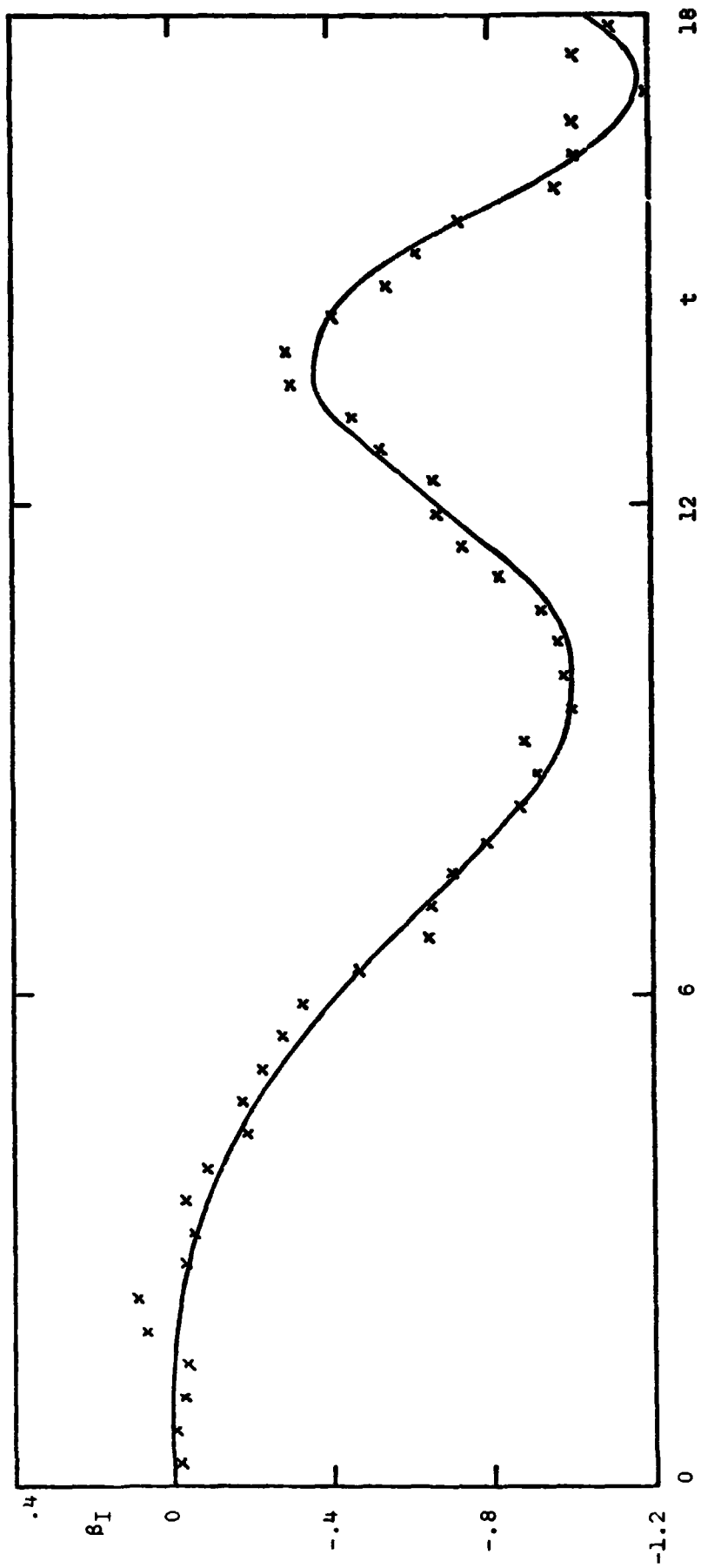
Fig. 5c, $\theta_I = u(t)$, Model (e)

Fig. 6a

Fig. 6b

Fig. 6c

Fig. 6d

Fig. 7a

v_I

Fig. 7b

Fig. 7c

RELAT. PARAMETER
STD. DEVIATION

TIME (NON-DIMENSIONAL)

Fig. 8